Aperiodic quantum *XXZ* chains: Renormalization-group results

André P. Vieira*
Instituto de Física da Universidade de São Paulo, Caixa Postal 66318, 05315-970, São Paulo, Brazil
(Received 20 November 2004; published 12 April 2005)

We report a comprehensive investigation of the low-energy properties of antiferromagnetic quantum *XXZ* spin chains with aperiodic couplings. We use an adaptation of the Ma-Dasgupta-Hu renormalization-group method to obtain analytical and numerical results for the low-temperature thermodynamics and the ground-state correlations of chains with couplings following several two-letter aperiodic sequences, including the quasiperiodic Fibonacci and other precious-mean sequences, as well as sequences inducing strong geometrical fluctuations. For a given aperiodic sequence, we argue that in the easy-plane anisotropy regime, intermediate between the *XX* and Heisenberg limits, the general scaling form of the thermodynamic properties is essentially given by the exactly known *XX* behavior, providing a classification of the effects of aperiodicity on *XXZ* chains. We also discuss the nature of the ground-state structures and their comparison with the random-singlet phase characteristic of random-bond chains.

DOI: 10.1103/PhysRevB.71.134408 PACS number(s): 75.10.Jm, 75.50.Kj

I. INTRODUCTION

At low temperatures, the interplay between lack of translational invariance and quantum fluctuations in low-dimensional strongly correlated electron systems may induce novel phases with peculiar behavior. In particular, randomness in quantum spin chains may lead to Griffiths phases,[1,2] random quantum paramagnetism,[3–5] large-spin formation,[6,7] and random-singlet phases.[8,9] On the other hand, studies on the influence of deterministic but aperiodic elements on similar systems (see, e.g., Refs. 10–18), inspired by the experimental discovery of quasicrystals,[19] have revealed strong effects on dynamical and thermodynamic properties, although much less is known concerning the precise nature of the underlying ground-state phases.[20]

Prototypical models for those studies are spin-$\frac{1}{2}$ antiferromagnetic *XXZ* chains described by the Hamiltonian

$$H = \sum_i J_i (S_i^x S_{i+1}^x + S_i^y S_{i+1}^y + \Delta S_i^z S_{i+1}^z), \tag{1}$$

where $J_i > 0$ and the S_i are spin operators. In the uniform case ($J_i \equiv J$), the ground state for chains with $-1 < \Delta \leqslant 1$ is critical,[21] exhibiting power-law decay of the pair correlations as a function of the distance between spins,[22] as well as gapless elementary excitations. Such a critical phase is unstable towards dimerization, i.e., the introduction of alternating couplings J_{odd} and J_{even}, in the presence of which a gap opens between the (now localized) ground state and the first excited states.[23–25] This instability hints at the profound effects produced by fully breaking the translational symmetry of the system.

Random-bond versions of these chains have been much studied by a real-space renormalization-group (RG) method introduced[26,27] by Ma, Dasgupta, and Hu (MDH) for the Heisenberg chain ($\Delta = 1$) and more recently extended by Fisher,[1,2,8] who gave evidence that the method becomes asymptotically exact at low energies. In the last few years, the method has been applied and adapted to a variety of random systems (see, e.g., Refs. 6, 7, and 28–34). The basic idea is to decimate the spin pairs coupled by the strongest bonds (those with the largest gaps between the local ground state and the first excited multiplet), forming singlets and inducing weak effective couplings between neighboring spins, thereby reducing the energy scale. For *XXZ* chains in the regime $-\frac{1}{2} < \Delta \leqslant 1$, the method predicts the ground state to be a random-singlet phase, consisting of arbitrarily distant spins forming rare, strongly correlated singlet pairs.[8]

Another way of breaking the translational symmetry is suggested by analogies with quasicrystals. These are structures which exhibit symmetries forbidden by traditional crystallography, and which correspond to projections of higher dimensional Bravais lattices onto low-dimensional subspaces.[35] A one-dimensional example is provided by the Fibonacci quasiperiodic chain, obtained from a cut-and-project operation on a square lattice.[36] In this chain, the spins are separated by two possible distances, *a* and *b*, whose sequence, starting from the left end of the chain, is *abaab*…. This sequence can be generated by repeatedly applying a substitution (or inflation) rule $a \to ab$, $b \to a$, starting from a single distance *a*. Associating with each *a* a coupling J_a and with each *b* a coupling J_b we obtain a spin chain with couplings following a Fibonacci sequence. More generally, we can postulate a two-letter substitution rule, build the corresponding letter sequence, and associate couplings with letters to obtain spin chains whose couplings follow aperiodic but deterministic sequences.[37] Quasiperiodic sequences are characterized by a Fourier spectrum consisting of Bragg peaks, but more complex spectra (such as singular-continuous) can be generated by substitution rules.[38] In this work we apply the term "aperiodic" when referring to nonperiodic, self-similar sequences, also encompassing those that are strictly quasiperiodic in the above sense.

In *XX* spin chains ($\Delta = 0$), the low-temperature thermodynamic behavior can be qualitatively determined for virtually any aperiodic sequence by an exact RG method.[17] The effects of aperiodicity depend on the topological properties of the sequence. If the fraction of letters *a* (or *b*) at odd positions is different from that at even positions (i.e., if there is

average dimerization), then a finite gap opens between the global ground state and the first excited states, and the chain becomes noncritical. Otherwise, the scaling of the lowest gaps can be classified according to the wandering exponent ω measuring the geometric fluctuations g related to nonoverlapping pairs of letters,[17] which vary with the system size N as $g \sim N^{\omega}$. If $\omega < 0$, aperiodicity has no effect on the long-distance, low-temperature properties, and the system behaves as in the uniform case, with a finite susceptibility at $T=0$. If $\omega=0$, as in the Fibonacci sequence, aperiodicity is marginal and may lead to nonuniversal power-law scaling behavior of the thermodynamic properties. If $\omega>0$, aperiodicity is relevant in the RG sense, affecting the $T=0$ critical behavior and leading to exponential scaling of the lowest gaps Λ at long distances r, according to the form $\Lambda \sim \exp(-r^{\omega})$. In particular, for sequences with $\omega=\frac{1}{2}$, the geometric fluctuations mimic those induced by randomness, and the scaling behavior is similar to the one characterizing the random-singlet phase.[8]

In contrast, results for the effects of aperiodicity on low-energy properties of *XXZ* chains have been so far scarce and restricted to particular sequences. Vidal, Mouhanna, and Giamarchi[13,14] studied the related problem of an interacting spinless fermion chain with Fibonacci or precious-mean potential by using bosonization techniques, which are valid in the weak-modulation regime ($J_a \simeq J_b$). At half filling, where the system corresponds to an *XXZ* chain in zero external field, their calculations predict that aperiodicity will drive the system away from the usual Luttinger-liquid behavior for $0 \leqslant \Delta \leqslant 1$. A similar conclusion is drawn from studies on a Hubbard chain with hoppings following a Fibonacci sequence.[16] Density-matrix renormalization-group (DMRG) results on *XXZ* chains with precious-mean couplings,[15] and recent real-space RG calculations on the Fibonacci *XXZ* chain[39,40] (also based on the MDH scheme), likewise predict that low-temperature properties are different than in the uniform chains. The zero-temperature magnetization curve of Fibonacci *XXZ* chains has also been investigated,[18] with emphasis on determining the plateau structure.

Our aim in this paper is to investigate the effects of *arbitrary* aperiodic coupling distributions on the low-temperature properties of *XXZ* chains, reinforcing and extending our previous results.[41] From an adaptation of the Ma-Dasgupta-Hu RG scheme, we obtain information about low-temperature thermodynamics and ground-state correlation functions for several aperiodic sequences. Our results, which are presumably exact in the strong-modulation limit ($J_a \ll J_b$ or $J_a \gg J_b$), point to the following conclusions:

(1) The exact classification found in the *XX* limit can arguably be extended to *XXZ* chains in the anisotropy regime $0 < \Delta \leqslant 1$. We predict that dimerized aperiodicity opens a gap to the lowest excitations, and that otherwise the effects of aperiodicity on the low-temperature thermodynamics are gauged by the same exponent ω, irrespective of anisotropy. In particular, sequences which are strictly marginal in the *XX* limit continue to be so for anisotropies $0 < \Delta < 1$, but may be marginally relevant in the Heisenberg limit.

(2) On the other hand, ω is found not to define the behavior of correlation functions, although ground-state structures in the presence of marginal or relevant couplings also reflect self-similar properties of the sequences. Dominant correlations correspond to well defined distances, related to the rescaling factor of the sequences (contrary to the random-singlet phase, where no such characteristic distances exist), and two types of behavior are possible; either the chains can be decomposed into a hierarchy of singlets, forming a kind of "aperiodic-singlet phase," or into a hierarchy of effective spins, in which case low-energy excitations involve an exponentially large number of spins. This is in sharp contrast both to the gapless spin-wave excitations of the uniform chains and to the gapped triplet-wave excitations of the dimerized chains.

(3) Based on second-order calculations, the long-distance decay exponents of average ground-state correlation functions are seen to vary with the coupling ratio in the presence of strictly marginal aperiodicity. Otherwise, strong universality (i.e., independence of the exponents on both the coupling ratio and anisotropy) is obtained for the whole line $0 \leqslant \Delta < 1$, although different decay exponents may emerge in the Heisenberg limit. Also, the scaling form of typical (rather than average) correlations follows essentially the same scaling form as the energy gaps, similarly to what happens for random-bond chains.

In order to make the paper self-contained, we begin by reviewing some known results. So, in Sec. II we present the basics of the Ma-Dasgupta-Hu scheme, as applied to random-bond *XXZ* chains, and summarize the properties of the underlying random-singlet phase. Also, in Sec. III we provide a short discussion on aperiodic sequences, as well as a sketch of the exact RG results for *XX* chains with aperiodic couplings. Our adaptation of the Ma-Dasgupta-Hu method to aperiodic *XXZ* chains is described in Sec. IV, and results for marginal and relevant aperiodicities are presented in Secs. V and VI. Section VII is devoted to a discussion and conclusions. There are also two appendices, in which some important technical points are detailed.

II. RANDOM-BOND SPIN CHAINS AND THE MA-DASGUPTA-HU METHOD

Consider an antiferromagnetic quantum spin-$\frac{1}{2}$ chain described by the Hamiltonian

$$H = \sum_i J_i (S_i^x S_{i+1}^x + S_i^y S_{i+1}^y + \Delta_i S_i^z S_{i+1}^z), \tag{2}$$

where $J_i > 0$ and all anisotropies are such that $0 \leqslant \Delta_i \leqslant 1$. Let us assume that the couplings J_i are randomly distributed according to a broad probability distribution $\wp(J_i)$ having an upper cutoff $J_{\max}$. Under such conditions, in a finite but large chain, there is a strongest bond $J_0 \simeq J_{\max}$ connecting, say, spins S_1 and S_2, which in turn are coupled to their other nearest-neighbors S_l and S_r by weaker bonds J_l and J_r. The local Hamiltonian connecting S_1 and S_2 is

$$H_0 = J_0 (S_1^x S_2^x + S_1^y S_2^y + \Delta_0 S_1^z S_2^z),$$

whose ground state is a singlet, separated from the first excited states by an energy gap $\Lambda_0 = \frac{1}{2}(1+\Delta_0) J_0$. The idea behind the Ma-Dasgupta-Hu[26,27] method is that, at tempera-

tures below Λ_0, S_1 and S_2 can be decimated out of the system, since they couple into a singlet, giving a negligible contribution to the thermodynamic properties. Nevertheless, their virtual excitations induce a weak effective coupling between S_l and S_r, described by the Hamiltonian

$$H' = J'(S_l^x S_r^x + S_l^y S_r^y + \Delta' S_l^z S_r^z).$$

The parameters J' and Δ' can be obtained by second-order perturbation theory (see Appendix A) and are given by

$$J' = \frac{1}{1+\Delta_0}\frac{J_l J_r}{J_0} \quad \text{and} \quad \Delta' = \frac{1+\Delta_0}{2}\Delta_l \Delta_r. \tag{3}$$

Notice that J' is smaller than either J_l, J_r or J_0; likewise, unless all $\Delta_i = 1$, the effective anisotropy Δ' is smaller than either Δ_l or Δ_r. Thus, after eliminating S_1 and S_2, the overall energy scale is reduced. The previous steps can be repeated with the next largest bond, which most probably is not J'.

Starting from Eqs. (3) Fisher[8] was able to write and solve recursion relations for the probability distribution of the effective couplings. The fixed-point distribution is presumably independent of the initial couplings,[42] and it diverges as a power law for $J' \to 0^+$, indicating that the perturbative approach leading to Eqs. (3) becomes essentially exact for asymptotically low energies.

The ground state is a "random-singlet" phase, consisting of arbitrarily distant spins forming rare, strongly correlated singlet pairs.[8,43] Exciting a singlet whose spins are separated by a distance r costs an energy of order Λ, with a dynamic scaling form

$$\Lambda \sim e^{-\mu\sqrt{r/r_0}},$$

where μ and r_0 are constants. At low temperatures, the zero-field susceptibility diverges as

$$\chi \sim \frac{1}{T \ln^2 T}.$$

Average ground-state correlations are dominated by the rare singlet pairs, and they decay as a power law,

$$C(r) \equiv \left|\overline{\langle \mathbf{S}_i \cdot \mathbf{S}_{i+r}\rangle}\right| \sim \frac{1}{r^2},$$

where the bar denotes an average over the whole chain, while typical correlations are short-ranged, following

$$C_{\text{typ}}(r) \sim e^{-\mu_{\text{typ}}\sqrt{r/r_0}}.$$

These asymptotic results are independent of the anisotropies Δ_i, as long as $0 \leqslant \Delta_i \leqslant 1$ for all i, with the same distribution on even and odd bonds.

III. APERIODIC SEQUENCES AND *XX* CHAINS

Following closely the analysis of Hermisson,[17] in this section we consider antiferromagnetic quantum *XX* chains, described by the Hamiltonian

$$H = \sum_i J_i (S_i^x S_{i+1}^x + S_i^y S_{i+1}^y), \tag{4}$$

where now the strengths of the site-dependent couplings J_i can be either J_a or J_b and are distributed according to deterministic but aperiodic binary sequences, obtained by substitution (or inflation) rules of the form

$$\sigma: \begin{cases} a \to w_a \\ b \to w_b, \end{cases}$$

where w_a and w_b are words (finite strings) composed of letters a and b. A well known example is provided by the Fibonacci sequence, whose substitution rule is

$$\sigma_{\text{fb}}: \begin{cases} a \to ab \\ b \to a. \end{cases}$$

Starting from a single letter a, repeated application of σ_{fb} yields strings with lengths given by the Fibonacci numbers 1, 2, 3, 5, 8,…, ultimately producing a letter sequence *abaababaaba*…, for which no period can be identified.

Given an inflation rule σ, various statistical properties[44] of the associated sequence are enclosed in the substitution matrix,

$$\mathbf{M} = \begin{pmatrix} \#_a(w_a) & \#_a(w_b) \\ \#_b(w_a) & \#_b(w_b) \end{pmatrix},$$

where $\#_a(w_b)$ denotes the number of letters a in the word w_b. The largest eigenvalue of $\mathbf{M}$, λ_+, gives the asymptotic scaling factor of the string length (i.e., the ratio between the lengths of the strings corresponding to successive iterations of the rule σ); the entries of the corresponding eigenvector are proportional to the frequencies p_a and p_b of letters a and b in the limit (infinite) sequence.

The remaining eigenvalue, λ_-, is related to the geometric fluctuations of the sequence, which are defined in the following way. Let N_n^a be the number of letters a in the string obtained after n iterations of σ, and N_n be the corresponding total number of letters (the length of the string). Then, a measure of the geometric fluctuations induced by the sequence is the difference g_n between N_n^a and the number of letters a expected from the limit-sequence frequency p_a, and this behaves as

$$g_n = |N_n^a - p_a N_n| \sim |\lambda_-|^n.$$

Since $N_n \sim \lambda_+^n$, this last equation can be rewritten as

$$g_n \sim N_n^{\omega_l},$$

by defining the "wandering exponent,"

$$\omega_l = \frac{\ln|\lambda_-|}{\ln \lambda_+}.$$

If $\omega_l < 0$, fluctuations become smaller as the string grows, and the sequence looks more and more "periodic." On the other hand, if $\omega_l > 0$, fluctuations increase without limit. The marginal case $\omega_l = 0$ is in general connected to logarithmic fluctuations. It can be shown[45] that substitutions for which

$\omega_l < 0$ generate quasiperiodic (or limit-quasiperiodic) sequences.

The concept of geometric fluctuations is essential in establishing the Harris-Luck criterion[46,47] for the relevance of inhomogeneities to the critical behavior of magnetic systems. The criterion states that, if fluctuations in the local parameters controlling the criticality of the system vary with some characteristic length L as $g \sim L^{\omega}$, then there is a critical value of the exponent ω above which the presence of inhomogeneities can affect the critical behavior. This happens for

$$\omega > 1 - \frac{1}{d\nu}, \tag{5}$$

where d is the number of dimensions along which inhomogeneities are distributed, and ν is the correlation-length critical exponent of the underlying uniform system. Randomly distributed inhomogeneities lead to $\omega = \frac{1}{2}$, and the general Harris criterion[46,48,49] is recovered.

The ground state of the model in Eq. (4) is critical in the uniform limit ($J_i \equiv J$): there is no energy gap to the low-lying excitations, and pair correlations decay as power laws,[50]

$$C^{\alpha\alpha}(r) = \left|\overline{\langle S_i^{\alpha} S_{i+r}^{\alpha}\rangle}\right| \sim r^{-\eta^{\alpha\alpha}},$$

with $\eta^{xx} = \eta^{yy} = \frac{1}{2}$ and $\eta^{zz} = 2$. This phase is unstable towards dimerization (i.e., the presence of couplings J_o and J_e alternating between odd and even bonds), in which case a gap opens in the low-energy spectrum, and ground-state correlations become short-ranged. More generally, the model exhibits a (zero-temperature) quantum phase transition between two dimer phases for[17,51]

$$\delta = \overline{\ln J_{2j-1}} - \overline{\ln J_{2j}} = 0. \tag{6}$$

If $J_{2j-1} \equiv J_o$ and $J_{2j} \equiv J_e$, the phase transition occurs for $\delta = \ln(J_o/J_e) = 0$, and belongs to the Onsager universality class, with $\nu = 1$.

When the couplings J_i are chosen according to aperiodic sequences for which the fractions of letters a (or b) at even and odd positions are different, Eq. (6) is not satisfied, and the system is in a dimer phase. This suggests that the local parameters defining the criticality of XX chains are the shifts $\delta_j = \ln(J_{2j-1}/J_{2j})$. In order to study the fluctuations of the δ_j, which depend on two consecutive couplings, we must usually consider the sequence of nonoverlapping letter pairs associated with a given aperiodic sequence. To build the inflation rule $\sigma^{(2)}$ for such pairs, it is necessary to iterate the original rule σ until the strings obtained from a single a and b have lengths of the same parity. As an illustration, let us take the Fibonacci sequence. Applying σ_{fb} three times yields

$$\sigma_{\mathrm{fb}}^{3}: \begin{cases} a \to abaab \\ b \to aba. \end{cases}$$

Noting that the pair bb does not occur in the sequence, we readily obtain

$$\sigma_{\mathrm{fb}}^{(2)}: \begin{cases} aa \to (ab)(aa)(ba)(ba)(ab) \\ ab \to (ab)(aa)(ba)(ba) \\ ba \to (ab)(aa)(ba)(ab). \end{cases}$$

For a general pair inflation rule $\sigma^{(2)}$, we can define an associated substitution matrix,

$$\mathbf{M}^{(2)} = \begin{pmatrix} \#_{aa}(w_{aa}) & \#_{aa}(w_{ab}) & \#_{aa}(w_{ba}) & \#_{aa}(w_{bb}) \\ \#_{ab}(w_{aa}) & \#_{ab}(w_{ab}) & \#_{ab}(w_{ba}) & \#_{ab}(w_{bb}) \\ \#_{ba}(w_{aa}) & \#_{ba}(w_{ab}) & \#_{ba}(w_{ba}) & \#_{ba}(w_{bb}) \\ \#_{bb}(w_{aa}) & \#_{bb}(w_{ab}) & \#_{bb}(w_{ba}) & \#_{bb}(w_{bb}) \end{pmatrix},$$

where now $\#_{ab}(w_{ba})$ denotes the number of pairs ab in the word associated with the pair ba. The leading eigenvalues λ_1 and λ_2 of $\mathbf{M}^{(2)}$ define another wandering exponent,

$$\omega = \frac{\ln|\lambda_2|}{\ln \lambda_1},$$

which governs the fluctuations of the letter pairs, and consequently of the δ_j. It is essential to note that ω is in general different from ω_l: for the Fibonacci sequence, for instance, we have $\omega_l = -1$, but $\omega = 0$. (There are aperiodic sequences, generated by what Hermisson called mixed substitution rules, for which a pair inflation rule cannot be defined; however, it is still possible to investigate the fluctuations of the δ_j in terms of a set of substrings with minimal length.)

By an exact renormalization-group treatment, Hermisson[17] was able to build recursion relations for effective couplings and to show that, in agreement with the above heuristic argument, the eigenvalues λ_i of $\mathbf{M}^{(2)}$ give directly the RG eigenvalues y_i around the uniform fixed point of XY chains with aperiodic couplings,

$$y_i = \frac{\ln|\lambda_i|}{\ln \lambda_1},$$

while the corresponding eigenvectors yield the scaling fields. Thus, aperiodicity is relevant in the RG sense (i.e., it moves the RG flows away from the uniform fixed point) if the next-to-leading eigenvalue $y_2 = \omega$ is positive, exactly as predicted by the Harris-Luck criterion, Eq. (5), with $d = \nu = 1$. (To be precise, the eigenvalue of $\mathbf{M}^{(2)}$ entering the definition of ω is not always the next-to-leading one, but rather the second-largest eigenvalue whose corresponding scaling field is nonzero for a generic choice of coupling constants.)

For a large class of aperiodic sequences fulfilling Eq. (6), λ_2 is given in the XX limit by an integer k. When a pair substitution rule can be defined, this integer is simply given by

$$k = \#_{ab}(w_{ab}) - \#_{ba}(w_{ab}).$$

Thus, the wandering exponent in the XX limit is of the form

$$\omega = \frac{\ln k}{\ln \tau}, \tag{7}$$

where $\tau \equiv \lambda_1$ corresponds to the rescaling factor of the sequence of letter pairs.

It is also possible to determine the scaling of the lowest energy levels Λ with the system size r. For irrelevant or marginal aperiodicity ($\omega \leqslant 0$) we have

$$\Lambda \sim r^{-z}, \tag{8}$$

with a dynamical exponent z equal to unity if $\omega<0$, but which can vary with the coupling ratio J_a/J_b in the marginal cases ($\omega=0$). Relevant aperiodicity ($\omega>0$) leads to a different scaling form,

$$\Lambda \sim \exp(-\mu r^{\omega}), \quad (\mu = \text{const}) \tag{9}$$

and to a formally infinite dynamical exponent. From Eqs. (8) and (9), scaling forms for low-temperature thermodynamic properties, such as the specific heat and zero-field susceptibility, can be obtained, as discussed in the next sections. Ground-state correlation functions, however, do not seem to be simply accessible from the exact RG treatment.

Since the critical phase of uniform *XXZ* chains is also unstable towards dimerization in the whole anisotropy regime $0<\Delta\leqslant 1$, one might expect that the relevant geometrical fluctuations in the presence of aperiodic couplings would be somehow related to the δ_j defined above. (A precise definition of the relevant local parameters would require a generalization of the criticality condition [Eq. (6)] to *XXZ* chains, which, to the best of our knowledge, is not currently available.) Consequently, the exponent ω would be involved in determining the scaling behavior of thermodynamic properties of aperiodic chains for all anisotropies intermediate between the *XX* and Heisenberg limits. The results of the next sections indeed provide evidence that this seems to be the case.

IV. THE MA-DASGUPTA-HU METHOD FOR APERIODIC *XXZ* CHAINS

We now wish to investigate the effects of aperiodic couplings on *XXZ* chains described by the Hamiltonian in Eq. (2). Based on the success of the Ma-Dasgupta-Hu scheme in predicting the properties of random-bond chains, we expect that it also works in the presence of aperiodicity. We concentrate on the case of uniform anisotropy ($\Delta_i \equiv \Delta$), but more general situations can be considered.

Applying the MDH method to aperiodic chains requires taking into account that now, since we have only two distinct coupling constants, there are many spin blocks with the same (largest) gap at a given energy scale. Also, those blocks may consist of more than two spins, in which case effective spins would form upon renormalization. The strategy is to sweep through the lattice until all blocks with the same gap have been renormalized, leading to new effective couplings (and possibly spins). Then we search for the next largest gap, which again corresponds to many blocks. When all possible original blocks have been considered, there remain some unrenormalized spins, possibly along with effective ones, defining new blocks which form a second generation of the lattice. The process is then iterated, leading to the renormalization of the spatial distribution of effective blocks (or bonds) along the generations.

Due to the self-similarity inherent to aperiodic sequences generated by inflation rules, it is natural that the block distribution reaches a periodic attractor (usually a fixed point or a two-cycle) after a few lattice sweeps; numerical implementations of the method indicate that this attractor is independent of the anisotropy Δ for all coupling ratios. By studying recursion relations for the effective couplings, we can obtain analytical results. As the RG steps proceed, the coupling ratio usually gets smaller, suggesting that the method becomes asymptotically exact. This picture holds for marginal ($\omega=0$) and relevant ($\omega>0$) aperiodicity. Irrelevant aperiodicity is characterized by a wandering exponent $\omega<0$, meaning that geometric fluctuations become negligible at long distances. An example is provided by the Thue-Morse sequence, generated by the substitution rule $a\rightarrow ab$, $b\rightarrow ba$, for which $\omega=-\infty$. Applying the MDH scheme to the Thue-Morse sequence leads to an effective coupling ratio which approaches unity along the generations, although the couplings themselves become smaller. This means that the perturbative approach in the core of the MDH scheme eventually breaks down, and no asymptotic behavior can be obtained. However, this intuitively agrees with the picture that irrelevant aperiodicity leads to the same critical properties as the uniform model, where all couplings have the same value.

For sequences where the fraction of letters a (or b) at odd bonds is different from that at even bonds (i.e., where the sequence induces average dimerization), one generally expects that a finite gap opens between the global ground state and the first excited states, independent of the value of the wandering exponent ω. This is the case of the period-doubling sequence, built from the substitution rule $a\rightarrow ab$, $b\rightarrow aa$. Upon application of the MDH method, after a few lattice sweeps (with the precise number depending on the strength of dimerization) we reach a situation where, say, all strong bonds occupy even positions, whereas all bonds at odd positions are weaker. Thus, all remaining couplings are necessarily decimated in a last lattice sweep, generating a final effective coupling which approaches zero exponentially with the system size N. This can be interpreted as indicating that there is no correlation between spins separated by large distances, in agreement to what happens in gapped Heisenberg and *XX* chains. In the presence of average dimerization, few quantitative predictions can be drawn from the MDH method; one of them is an estimate of the excitation gap, whose order of magnitude is provided by the value of the strong bonds in the final lattice sweep. In contrast, randomly dimerized Heisenberg chains in the strong-randomness limit are in a gapless Griffiths phase, exhibiting short-range correlations but a diverging susceptibility.[28]

In a general situation, the blocks to be renormalized consist of n spins connected by equal bonds J_0, and coupled to the rest of the chain through weaker bonds J_l and J_r. As discussed in Appendix A, the ground state for blocks with an even number of spins is a singlet (as in the original MDH method), and at low energies we can eliminate the whole block, along with J_l and J_r, leaving an effective antiferromagnetic bond J' coupling the two spins closer to the block and given by second-order perturbation theory as

$$J' = \gamma_n \frac{J_l J_r}{J_0} \quad (n \text{ even}),$$

with Δ-dependent coefficients γ_n. On the other hand, a block with an odd number of spins has a doublet as its ground

state; at low energies, it can be replaced by an effective spin connected to its nearest neighbors by antiferromagnetic effective bonds

$$J'_{l,r} = \gamma_n J_{l,r} \quad (n \text{ odd}),$$

whose values are calculated by first-order perturbation theory.

In general, the anisotropy parameters are also renormalized and become site dependent; for n even, the effective anisotropy is $\Delta' = \delta_n(\Delta_0)\Delta_l\Delta_r$, while for n odd $\Delta'_{l,r} = \delta_n(\Delta_0)\Delta_{l,r}$, with $|\delta_n(\Delta)| < 1$ for $0 \leqslant \Delta < 1$ and $\delta_n(1) = 1$. So, for $0 < \Delta < 1$ the Δ_i flow to the *XX* fixed point (all $\Delta_i = 0$), ultimately reproducing the corresponding scaling behavior, while for the Heisenberg chain all Δ_i remain equal to unity. An analytical treatment of the intermediate anisotropy regime is possible (see Ref. 40), leading to a prediction of the effective coupling ratio for which the system crosses over to the *XX* behavior. However, for simplicity, we present analytical calculations for the *XX* and Heisenberg limits, showing some numerical results for the general case $0 \leqslant \Delta \leqslant 1$. If we start with a uniform anisotropy $\Delta > 1$, the Δ_i grow without limit, and the system ultimately behaves like an antiferromagnetic Ising chain, suppressing all quantum fluctuations. For $\Delta < 0$, the γ_n coefficients for n even become larger than unity, so that, if the modulation is not strong enough, the MDH scheme may produce effective couplings which are larger than the original couplings, leading to "bad" decimations; moreover, the two-spin local gap closes as $\Delta \to -1$. This puts the MDH results under suspicion, requiring a more careful analysis that is beyond the scope of the present work.

Correlation functions can be calculated at zeroth order by assuming that only spins which eventually appear in the same renormalized block are correlated. Note that an effective spin represents all spins in an original block via Clebsch-Gordan coefficients (see Appendix A), and this allows us to calculate correlations between any two spins whose effective spins end up in the same block at some stage of the RG process. In order to estimate correlations between other spin pairs we must expand the local ground states up to second order in $J_{l,r}/J_0$. This requires lengthy calculations (see Appendix B), and we restrict applications of this expansion to the simplest yet illustrative cases of sequences where only two-spin blocks are involved in the RG steps.

In Secs. V and VI, we present a detailed discussion of the results obtained by applying the MDH scheme to sequences inducing marginal or relevant aperiodicity.

We should mention that similar strong-modulation perturbative approaches have been applied to investigate the spectral properties of noninteracting electrons with aperiodic hopping parameters or single-site potentials (see, e.g., Refs. 52–54). However, the *XXZ* chain with nonzero anisotropy Δ is mapped by the Jordan-Wigner transformation onto a half-filled *interacting* electron system, for which, to the best of our knowledge, no such studies exist.

V. MARGINAL APERIODICITY

A. The Fibonacci sequence

First we apply the method to chains with Fibonacci couplings. This is the simplest example of the quasiperiodic

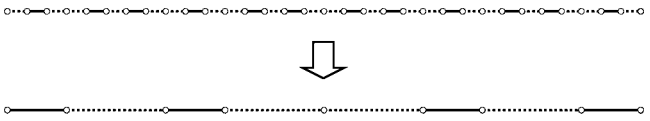

FIG. 1. Left end of the Fibonacci *XXZ* chain with $J_a < J_b$. Dashed (solid) lines represent weak (strong) bonds, while circles indicate the positions of the spins. Apart from a few bonds close to the chain ends, the effective couplings also form a Fibonacci sequence.

precious-mean sequences with marginal fluctuations.[17] A few bonds closer to the left end of the original chain, along with induced effective couplings, are shown in Fig. 1 for $J_a < J_b$. In this case, only singlets are formed by the RG process; apart from a few bonds close to the chain ends, the renormalized lattice is again a Fibonacci chain. An effective coupling J'_b is induced between spins separated by only one singlet pair, while J'_a connects spins separated by two singlet pairs, and in terms of the original couplings we have

$$J'_a = \gamma_2^2 \frac{J_a^3}{J_b^2} \quad \text{and} \quad J'_b = \gamma_2 \frac{J_a^2}{J_b}.$$

The bare coupling ratio is $\rho = J_a/J_b$; its renormalized value is $\rho' = \gamma_2\rho$. In each generation j, all decimated blocks have the same size r_j and gap Λ_j (proportional to the effective J_b bonds). The recursion relations for ρ and Λ are given by

$$\rho_{j+1} = \gamma_2\rho_j \quad \text{and} \quad \Lambda_{j+1} = \gamma_2\rho_j^2\Lambda_j. \tag{10}$$

For the *XX* chain $\gamma_2 = 1$, and thus $\rho_{j+1} = \rho_j$, corresponding to a line of fixed points. On the other hand, for the Heisenberg chain $\gamma_2 = \frac{1}{2}$, so that $\rho_{j+1} < \rho_j$, leading to a stable fixed point $\rho_\infty = 0$. Since the perturbative approach on which the MDH scheme is based works for $\rho \ll 1$, the method can be expected to yield asymptotically exact results for the Heisenberg Fibonacci chains. In both cases, solving Eqs. (10) gives the gap in the jth generation in terms of the original coupling ratio ρ and gap Λ,

$$\Lambda_j = \gamma_2^{j^2}\rho^{2j}\Lambda.$$

(Notice that, since γ_2 depends on the anisotropy, this last equation is valid only for $\Delta_i \equiv 0$ or $\Delta_i \equiv 1$; in the intermediate anisotropy regime, the variation of γ_2 along the generations must be taken into account.[40]) The distance between spins forming a singlet in the jth generation defines a characteristic length r_j, corresponding to the Fibonacci numbers $r_j = 1, 3, 13, 55, \ldots$; for $j \gg 1$ the ratio r_{j+1}/r_j approaches ϕ^3, where $\phi = (1+\sqrt{5})/2$ is the golden mean. So we have $r_j \sim r_0\phi^{3j}$, where r_0 is a constant, and we obtain the dynamical scaling relation,

$$\Lambda_j \sim r_j^{-\zeta} e^{-\mu \ln^2(r_j/r_0)}, \tag{11}$$

with $\zeta = -\frac{2}{3}\ln\rho/\ln\phi$ and $\mu = -\ln\gamma_2/9\ln^2\phi$. For the Heisenberg chain $(\gamma_2 = \frac{1}{2})$, Eq. (11) describes a weakly exponential scaling (with a formally infinite dynamical exponent), but not of the form $\Lambda \sim \exp(-r^\omega)$ found for the *XX* chain with relevant aperiodicity ($\omega > 0$). For the *XX* chain ($\gamma_2 = 1$), $\mu = 0$ and we can identify ζ with a dynamical exponent z,

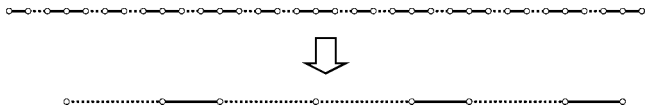

FIG. 2. Left end of the Fibonacci chains with $J_a > J_b$. Effective spins form in the first lattice sweep, giving rise to a Fibonacci chain with the roles of the weak and strong bonds interchanged, exactly as in the original lattice in Fig. 1.

whose value depends on the coupling ratio, leading to nonuniversal scaling behavior, characteristic of strictly marginal operators. (We can check that $z=\zeta$ corresponds to the asymptotic form of the exact *XX* expression[11,17] for $\rho \ll 1$.) This nonuniversality should hold in the anisotropy regime $0<\Delta<1$ with a "bare" value of ρ defined at a crossover scale. Note that, taking into account the scaling form $\Lambda \sim \exp(-r^{\omega})$ valid for relevant aperiodicity, we can view the above Heisenberg scaling form ($\mu \neq 0$) as a marginally relevant ($\omega \to 0^+$) case. The result in Eq. (11) has also been obtained in Ref. 39.

If we choose $J_a > J_b$, blocks with three spins connected by two strong bonds appear in the chain, producing effective spins upon renormalization. However, as illustrated in Fig. 2, the first lattice sweep yields again a Fibonacci chain with the roles of weak and strong bonds interchanged, exactly as in Fig. 1. The effective couplings in the second generation are given by

$$J_a' = \gamma_2 \gamma_3^2 \frac{J_b^2}{J_a} \quad \text{and} \quad J_b' = \gamma_3^2 J_b, \tag{12}$$

and the coupling ratio is now

$$\rho' = \frac{J_b'}{J_a'} = \frac{1}{\gamma_2}\frac{J_a}{J_b} = (\gamma_2 \rho)^{-1},$$

which is larger than one, showing that $J_a' < J_b'$. Thus, we can apply the same analysis as in the case with $J_a < J_b$, but now with bare couplings given by Eq. (12). So, in the *XX* chain, since $\gamma_2 = 1$, the MDH method predicts scaling forms which are symmetric under $\rho \to 1/\rho$, in agreement with the exact treatment.[11,17]

The susceptibility $\chi(T)$ can be estimated[8] by assuming that, at energy scale $\Lambda_j \sim T$, singlet pairs are effectively frozen, while unrenormalized spins are essentially free, contributing Curie terms to the susceptibility. Thus, if $n_j \sim r_j^{-1}$ is the number of surviving spins in the jth generation, $\chi(T \sim \Lambda_j) \sim n_{j+1}/\Lambda_j$. This already gives reasonable results, as indicated by comparison with those obtained for the *XX* chain from numerical diagonalization of finite chains,[39] based on the free-fermion method.[50] However, a more useful approximation can be obtained by noting that, in the jth generation, we can view the resulting lattice as composed of "independent" singlets in which a pair of spins is coupled via an *XXZ* interaction with effective bond and anisotropy parameters $J_b^{(j)}$ and $\Delta_b^{(j)}$. Since the fraction of such singlets with respect to the number of original bonds is $(n_j - n_{j+1})/2$, the free energy per site of the whole system, in the presence of an external field $h \to 0$, can be estimated as

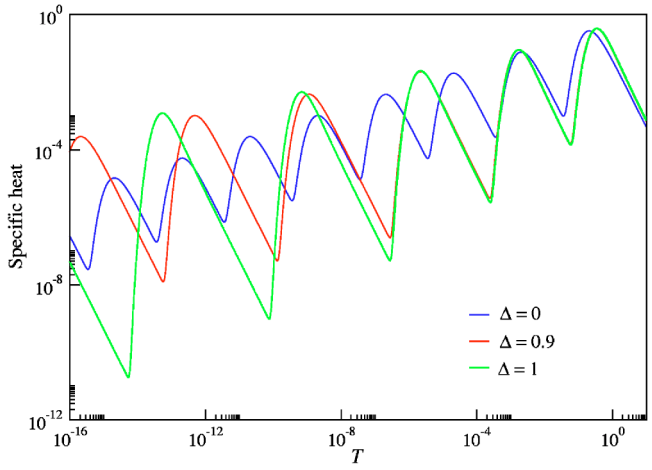

FIG. 3. (Color online) Specific heat of the Fibonacci *XXZ* chains for $J_a/J_b = \frac{1}{10}$ and three different values of the uniform anisotropy Δ, as given by the "independent-singlet" approximation.

$$f(h,T) = \frac{1}{2}\sum_j \frac{n_j - n_{j+1}}{2} F_{\text{pair}}\left(J_b^{(j)}, \Delta_b^{(j)}; h, T\right), \tag{13}$$

where $F_{\text{pair}}(J, \Delta; h, T)$ is the free energy of a pair of spins interacting via the Hamiltonian

$$H_{\text{pair}} = J(S_1^x S_2^x + S_1^y S_2^y + \Delta S_1^z S_2^z) - h(S_1^z + S_2^z).$$

Iterating the recursion relations for the effective couplings $J_{a,b}$ and $\Delta_{a,b}$, we can determine their values in each generation, and evaluate numerically the sum in Eq. (13) to obtain the free energy. Thermodynamic properties such as the zero-field susceptibility χ and the specific heat c can be obtained by the relations

$$\chi = -\left.\frac{\partial^2 f}{\partial h^2}\right|_{h=0} \quad \text{and} \quad c = -T\frac{\partial^2 f}{\partial T^2}.$$

As an example, Fig. 3 shows plots of the specific heat of Fibonacci *XXZ* chains with $J_a/J_b = \frac{1}{10}$ and three values of the anisotropy $\Delta = \Delta_a = \Delta_b$, corresponding to the *XX* and Heisenberg limits and to an intermediate case $\left(\Delta = \frac{9}{10}\right)$. The results for the *XX* limit agree very well with those obtained from numerical diagonalization, although the agreement becomes worse for larger coupling ratios; in particular, the specific-heat scaling law[11,17]

$$c(T) \sim T^{1/z} G_c\left(\frac{\ln T}{\ln \rho^2}\right),$$

with $z = \zeta(\rho)$ and G_c a function with period one, is fully satisfied, reflecting the strictly marginal character of the aperiodic perturbations. This is not the case in the Heisenberg limit, and the logarithmic amplitudes of the oscillations in the specific heat become larger with decreasing temperatures, reflecting the weakly exponential dynamical scaling in Eq. (11). For intermediate anisotropies, there is a crossover from Heisenberg-like to *XX*-like behavior as the temperature is lowered; the larger amplitude of the low-temperature oscillations corresponds to those of an *XX* chain with a bare coupling ratio $\rho_{\text{eff}} < \rho$ defined at a crossover scale in which ef-

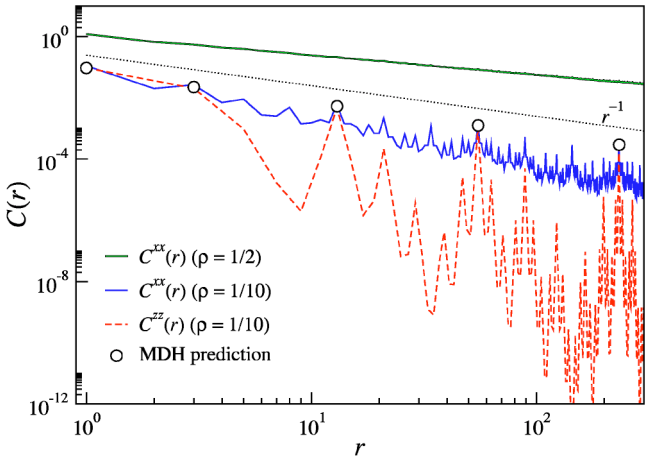

FIG. 4. (Color online) Ground-state correlations as a function of the distance between spins for the Fibonacci *XX* chain. The curves are obtained from numerical diagonalization of closed chains with 2584 sites. For $J_a/J_b=\frac{1}{10}$ (lower curves), dominant correlations correspond to distances $r_j=1$, 3, 13, 55 and 233, for which C^{xx} and C^{zz} are nearly equal, as predicted by the MDH method (circles), and decay as $1/r$ (dotted curve). Larger coupling ratios lead to a slower decay of C^{xx} (and a faster decay of C^{zz}), as seen for $J_a/J_b=\frac{1}{2}$ (upper curve, offset for clarity).

fective anisotropies become negligible. (For a detailed analysis, see Ref. 40.)

As all singlets formed in the jth generation have length r_j and the bond distribution is fixed, the average ground-state correlation between spins separated by a distance r_j can be estimated as

$$C^{\alpha\alpha}(r_j) \equiv \overline{\langle S_i^\alpha S_{i+r_j}^\alpha \rangle} \simeq \tfrac{1}{2}|c_0|(n_j - n_{j+1}) = \sigma|c_0| r_j^{-1}, \quad (14)$$

where the bar denotes an average over all possible pairs, σ is a constant, $\alpha=x,y,z$, and c_0 is the correlation between the two spins in a singlet, given by $c_0=-\frac{1}{4}$ for the Heisenberg chain and for both $\alpha=x$ and $\alpha=z$ in the *XX* chain. We point out that these should be the dominant correlations, and spins separated by distances other than r_j are predicted to be only weakly correlated. As shown in Fig. 4, results from numerical diagonalization for the *XX* Fibonacci chain with $\rho=\frac{1}{10}$ agree very well with the MDH predictions. Note that correlations in the uniform *XX* chain[50] decay as $C^{xx}(r)\sim r^{-1/2}$ and $C^{zz}(r)\sim r^{-2}$, so that dominant *xx* (*zz*) correlations in the Fibonacci chain are weaker (stronger) than in the uniform chain. Due to the strictly marginal character of the fluctuations induced by the aperiodic couplings, deviations from the predictions in Eq. (14) appear in the *XX* chain for larger values of ρ, as also shown in the figure. This point will be further discussed in the next subsection, but these deviations should not be present in the Fibonacci Heisenberg chain, where aperiodicity can be viewed as marginally relevant.

B. The silver-mean sequence

The silver-mean sequence is obtained from the substitution rule $a\to aab$, $b\to a$, and the rescaling factor predicted in the *XX* limit is[17]

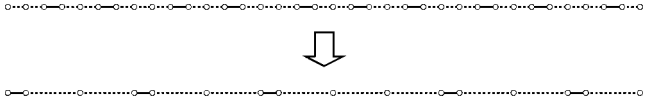

FIG. 5. Left end of the silver-mean chain with $J_a<J_b$. Effective couplings J_b' correspond to the original J_a bonds, while J_a' connects spins separated by one singlet pair. Apart from the leftmost bond, the effective couplings also form a silver-mean sequence.

$$\tau_{\rm sm} = 1 + \sqrt{2}.$$

When the MDH scheme is applied, the first lattice sweep also generates a silver-mean sequence, identical to the original one for $J_a<J_b$, but with the roles of weak and strong bonds interchanged for $J_a>J_b$, as shown in Figs. 5 and 6. In the latter case, the second-generation structure is identical to the third-generation lattice obtained for $J_a<J_b$, a situation we can assume without loss of generality. So, we can write the recursion relations

$$J_a' = \gamma_2 \frac{J_a^2}{J_b} \quad \text{and} \quad J_b' = J_a,$$

from which we get

$$\rho' \equiv \frac{J_a'}{J_b'} = \gamma_2 \frac{J_a}{J_b} \equiv \gamma_2 \rho \quad \text{and} \quad \frac{\Lambda'}{\Lambda} = \frac{J_b'}{J_b} = \rho.$$

These are similar to the relations found for the Fibonacci chains. The length of singlets formed in the jth generation is $r_j=1,1,3,7,17,41,\ldots$, whose asymptotic ratio is $r_{j+1}/r_j=\tau_{\rm sm}$. Thus, solving the recursion relations yields

$$\Lambda_j \sim r_j^{-\zeta(\rho)} e^{-\mu \ln^2(r_j/r_0)},$$

with

$$\zeta(\rho) = -\frac{\ln\left(\gamma_2^{-1/2}\rho\right)}{\ln \tau_{\rm sm}} \quad \text{and} \quad \mu = -\frac{\ln\left(\gamma_2^{1/2}\right)}{\ln^2 \tau_{\rm sm}}, \quad (15)$$

so that in the *XX* limit the scaling again corresponds to a nonuniversal power-law behavior with a dynamical exponent $z=\zeta(\rho)$.

As in the Fibonacci chains, pair correlations in the ground state can be estimated by noting that only singlets are produced by the RG process, and we conclude that for $\rho\ll 1$ the dominant correlations (those between spins separated by the characteristic distances $r_j=1,3,7,17,\ldots$) should behave as

$$C(r_j) \sim \frac{1}{r_j},$$

while correlations between spins separated by other distances should be negligible.

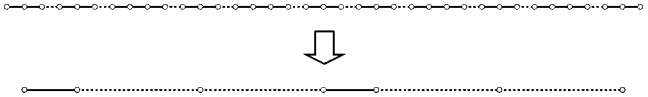

FIG. 6. Left end of the silver-mean chain with $J_a>J_b$. Effective spins form in the first lattice sweep, producing the same structure as the third generation for $J_a<J_b$.

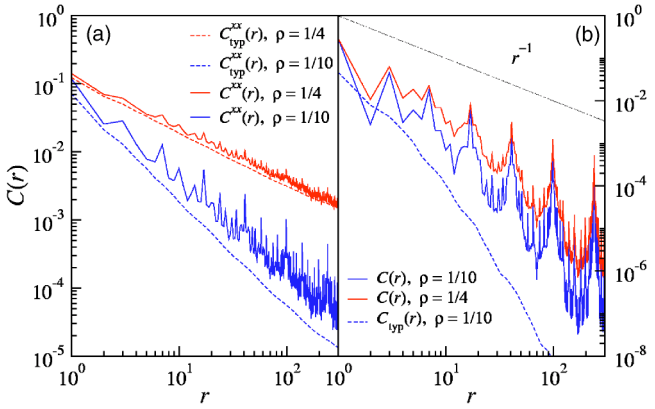

FIG. 7. (Color online) Ground-state pair correlations in the silver-mean *XX* (a) and Heisenberg (b) chains, for $\rho=\frac{1}{4}$ (upper curves) and $\rho=\frac{1}{10}$ (lower curves), obtained from the second-order MDH scheme (chains with 8119 sites). Solid and dashed curves correspond to average and typical correlations, respectively.

However, for *XX* chains, this is a rough approximation if the coupling ratio is not too small, and free-fermion calculations reveal a power-law decay of both $C^{xx}(r_j)$ and $C^{zz}(r_j)$ with ρ-dependent exponents, as in Fig. 4. This can be accounted for by the MDH method if we expand the ground-state vector to second order in ρ, as described in Appendix B. Results of such calculations are shown in Fig. 7 for $\rho=\frac{1}{4}$ and $\rho=\frac{1}{10}$, in the *XX* and Heisenberg limits. Both average and typical correlations are plotted; the latter, defined by

$$C^{\alpha\alpha}_{\rm typ}(r)=\exp\left(\overline{\ln|\langle S^{\alpha}_{i}S^{\alpha}_{i+r}\rangle|}\right),$$

filter out the contribution of those pairs of spins most strongly correlated, yielding an estimate of the correlation between two arbitrary spins separated by a distance r. In the random-singlet phase, characteristic of random-bond chains,[8] average correlations decay algebraically as $C(r)\sim 1/r^2$, whereas typical correlations are short-ranged, following $C_{\rm typ}(r)\sim\exp(-\sqrt{r/r_0})$. This is due to the fact that the average correlations are dominated by the rare singlet pairs, while the correlation between a typical pair of spins is of the order of some intermediate effective coupling (see Appendix B).

As shown in Fig. 7(a), this picture does not hold for silver-mean *XX* spin chains. As the coupling ratio is lowered, average and typical correlations exhibit clearly distinct behavior, but both $C^{xx}(r_j)$ and $C^{xx}_{\rm typ}(r)$ still follow approximately a power law, with ρ-dependent exponents, reproducing the results of the free-fermion calculations. This nonuniversality is related to the marginal character of the precious-mean fluctuations, which keeps the effective coupling ratio unchanged along the RG process, and can be qualitatively understood from the following argument. For each singlet pair coupled by a strong bond and whose spins are separated by a characteristic distance r_j, there exists a certain number of other spin pairs separated by the same distance r_j, but connected through weaker bonds, whose correlation (see Appendix B) is smaller than the strongest ones by factors of order ρ, ρ^2, ρ^3, etc. The average correlation can be estimated as

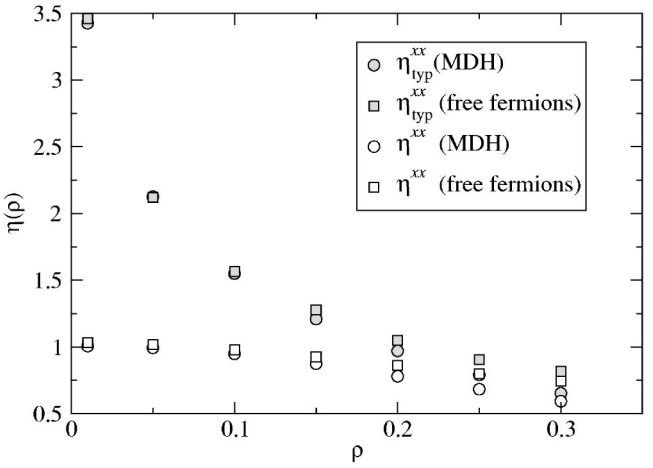

FIG. 8. Decay exponents of $C^{xx}(r_j)$ and $C^{xx}_{\rm typ}(r)$ for the *XX* silver-mean chain as a function of the coupling ratio $\rho=J_a/J_b$, obtained from both the second-order MDH scheme (chains with 8819 sites) and the free-fermion method (chains with 3363 sites). Errors bars are at most the same size as the symbols themselves.

$$C^{xx}(r_j)\sim(1+a_1\rho+a_2\rho^2+\cdots+a_j\rho^j)r_j^{-1}, \qquad (16)$$

where the a_n's are proportional to the fractions of pairs giving contributions of order ρ^n, and the sum has an upper cutoff at $n=j$, since r_j corresponds to the jth-generation singlets. Assuming that $a_n=a_1\alpha^{n-1}$, for some constant α (which can be numerically checked to be a reasonable approximation for small ρ), we have

$$1+a_1\rho+a_2\rho^2+\cdots+a_j\rho^j=1+\frac{1-(\alpha\rho)^j}{1-\alpha\rho}a_1\rho,$$

and taking into account that $r_j\sim r_0\tau_{\rm sm}^j$ we can write

$$(\alpha\rho)^j\sim r_j^{1-\eta(\rho)}, \quad \text{with} \quad \eta(\rho)=1-\frac{\ln(\alpha\rho)}{\ln\tau_{\rm sm}}.$$

Combining the above results we conclude that

$$C^{xx}(r_j)\sim\frac{1}{r_j},$$

for $\rho<\alpha^{-1}$, reproducing the zeroth-order MDH prediction, but a nonuniversal behavior,

$$C^{xx}(r_j)\sim\frac{1}{r_j^{\eta(\rho)}},$$

is obtained for $\rho>\alpha^{-1}$.

For the silver-mean *XX* chains, an estimate of the a_n based on numerical implementations of the MDH method gives $a_1\simeq 9.5$ and $\alpha\simeq 3$, but with some dependence on r_j and ρ. As shown in Fig. 8, the decay exponent η^{xx} of the average correlation approaches unity as $\rho\to 0$, but starts to decrease more rapidly for $\rho\gtrsim 0.1$, considerably less than $1/\alpha$; this discrepancy indicates that Eq. (16), with the assumption of constant a_n's, although providing a valuable insight into the origin of the nonuniversal behavior, is not a good approximation for larger coupling ratios. The exponents predicted by the second-order MDH scheme are systematically smaller

than the presumably exact ones obtained from the free-fermion method (which should tend to $\eta^{xx}=\frac{1}{2}$ as $\rho\to 1$). This also happens for the decay exponent $\eta^{xx}_{\rm typ}$ of the typical correlations, which diverges as $\rho\to 0$, in agreement with the fact that, in this limit, the chain decomposes into independent singlets. A similar behavior is observed for the transverse correlations $C^{zz}(r)$ and $C^{zz}_{\rm typ}(r)$ (but now the decay exponents approach $\eta^{zz}=\eta^{zz}_{\rm typ}=2$ as $\rho\to 1$).

On the other hand, dominant ground-state correlations in the Heisenberg silver-mean chain closely follow the predictions of the zeroth-order MDH scheme, as can be seen in Fig. 7(b). This is due to the fact that the effective coupling ratio decreases as the RG proceeds, and the contribution to $C(r_j)$ due to spin pairs other than those connected by strong bonds becomes exponentially negligible. Typical correlations decay not as a power law, but rather according to

$$C_{\rm typ}(r) \sim e^{-\mu_{\rm typ}\ln^2(r/r_0)},$$

precisely the same form of the dynamical scaling; by fitting the numerical results, the constant $\mu_{\rm typ}$ is found to be approximately $\mu/2$, with μ given by Eq. (15). As in the random-singlet phase, the scaling form of the typical correlations is similar to that of the lowest gaps, reflecting the fact that two spins separated by a distance r are basically uncorrelated until the energy scale is of order $\Lambda(r)$, when they become weakly correlated through an intervening spin taking part in a singlet pair.

C. The bronze-mean sequence

The bronze-mean sequence is built from the substitution rule $a\to aaab$, $b\to a$, with a large XX rescaling factor,[17]

$$\tau_{\rm bm}=\left(\frac{3+\sqrt{13}}{2}\right)^3\simeq 36.03.$$

The bond-distribution attractor produced by the MDH RG scheme is not a fixed point, but a two-cycle;[55] apart from a few bonds near the chain ends, the same distributions alternate between even and odd generations, as shown for $J_a<J_b$ in Fig. 9. In this case, the second-generation couplings relate to the original couplings by

$$\tilde{J}_a=\gamma_2^7\gamma_3^2\frac{J_a^5}{J_b^4}\quad\text{and}\quad \tilde{J}_b=\gamma_2^5\gamma_3^2\frac{J_a^4}{J_b^3}.$$

Likewise, in terms of the couplings in the previous generation, we write the third-generation couplings,

$$\tilde{J}_A=\gamma_3^2\gamma_4\frac{\tilde{J}_a^2}{\tilde{J}_b}\quad\text{and}\quad \tilde{J}_B=\gamma_3^2\tilde{J}_a,$$

and the fourth-generation couplings,

$$\tilde{J}'_a=\gamma_2^3\gamma_3^2\frac{\tilde{J}_A^4}{\tilde{J}_B^3}\quad\text{and}\quad \tilde{J}'_b=\gamma_2^2\gamma_3^2\frac{\tilde{J}_A^3}{\tilde{J}_B^2}.$$

Since the attractor is now a two-cycle, and not a fixed point, we must relate the couplings in the fourth and second generations. By eliminating $\tilde{J}_A$ and $\tilde{J}_B$ in the above equations, we get

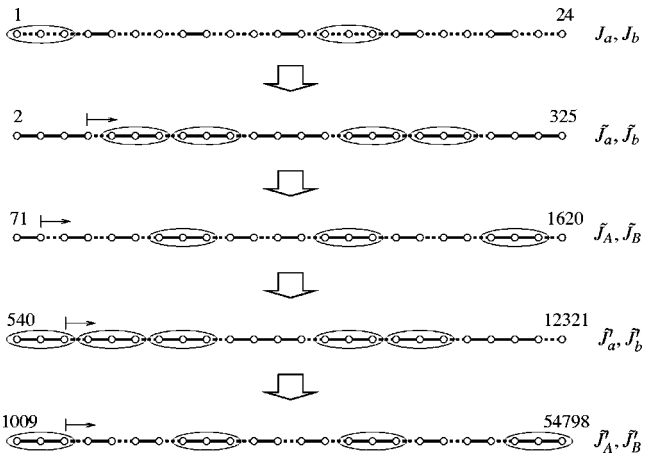

FIG. 9. First five generations of the bronze-mean XXZ chain with $J_a<J_b$, each showing the leftmost 24 sites. The numbers indicate the positions of the sites in the original chain. Encircled blocks contribute effective spins when renormalized. The labels on the right denote the effective bonds in each generation. The attractor of the block distribution is a two-cycle, reached at the second generation. All bonds to the right of the horizontal arrow follow the same sequence in the second (third) and fourth (fifth) generations.

$$\tilde{J}'_a=\gamma_2^3\gamma_3^4\gamma_4^4\frac{\tilde{J}_a^5}{\tilde{J}_b^4}\quad\text{and}\quad \tilde{J}'_b=\gamma_2^2\gamma_3^4\gamma_4^3\frac{\tilde{J}_a^4}{\tilde{J}_b^3},$$

so that the coupling ratios satisfy the recursion relation

$$\tilde{\rho}'\equiv\frac{\tilde{J}'_a}{\tilde{J}'_b}=\gamma_2\gamma_4\frac{\tilde{J}_a}{\tilde{J}_b}\equiv\gamma_2\gamma_4\tilde{\rho},$$

while the corresponding gaps are related by

$$\frac{\Lambda'}{\Lambda}=\frac{\tilde{J}'_b}{\tilde{J}_b}=\gamma_2^2\gamma_3^4\gamma_2^3\tilde{\rho}^4.$$

The distance between spins connected by strong bonds in the jth generation is $r_j=1,13,43,469,1549,\ldots$, which asymptotically gives $r_{j+2}/r_j=\tau_{\rm bm}$, so that $r_{2j}\sim r_0\tau_{\rm bm}^j$. Thus, solving the recursion relations for $\tilde{\rho}$ and Λ, and taking into account that $\tilde{\rho}=\gamma_2^2\rho$, we obtain the dynamic scaling form

$$\Lambda_{2j}=r_{2j}^{-\zeta(\rho)}\exp\left(-\mu\ln^2\frac{r_{2j}}{r_0}\right),\tag{17}$$

with

$$\zeta(\rho)=-\frac{\ln(\gamma_2^8\gamma_3^4\gamma_4\rho^4)}{\ln\tau_{\rm bm}}\quad\text{and}\quad \mu=-\frac{\ln(\gamma_2^2\gamma_4)}{\ln^2\tau_{\rm bm}}.$$

Of course, the same form is obtained if we choose to look at the odd generations. In the XX limit, as $\gamma_2=\gamma_4=1$, we again have $\mu=0$ and Eq. (17) corresponds to a nonuniversal power-law scaling behavior, with a dynamical exponent $z=\zeta(\rho)$; once more, as in all marginal XX chains, ζ equals the leading term in the $\rho\ll 1$ expansion of the exact dynamical exponent.[17] As in the Fibonacci and silver-mean chains, choosing $J_a>J_b$ leads to the same scaling behavior, since

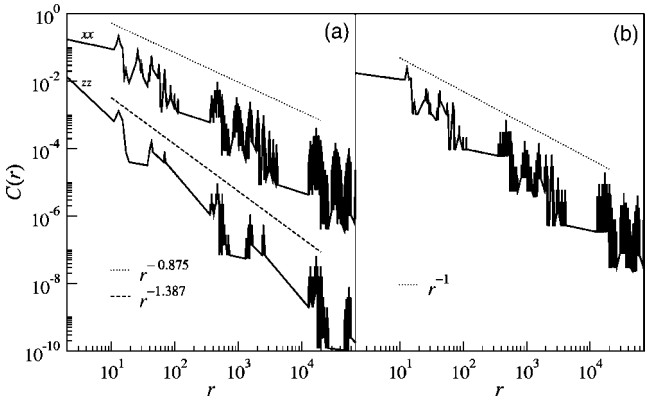

FIG. 10. Ground-state correlation functions of the *XX* (a) and Heisenberg (b) bronze-mean chains, obtained from the zeroth-order MDH scheme (chains with 2 010 601 sites).

after the first lattice sweep the bond distribution is essentially equal to the one obtained for $J_a < J_b$.

Thus, the bronze-mean chains present qualitatively the same low-temperature thermodynamic behavior as the Fibonacci chain. However, this is not the case for ground-state properties. As indicated in Fig. 9, the renormalization process in each generation involves all spins in the chain and gives rise to a hierarchy of effective spins, analogous to that shown in Fig. 11. As a consequence, an effective spin in the jth generation represents 3^{j-1} real spins. So, while the ground states of the Fibonacci and silver-mean chains could be described as "aperiodic-singlet phases," from which excitations of a given energy involve spins separated by a single, well defined distance, low-energy excitations in the bronze-mean chain involve an exponentially large number of spin pairs, whose distances are distributed in an increasing range. This is reflected in the ground-state correlation functions, which exhibit a fractal-like structure, as seen in Fig. 10. The strongest correlations in the chains correspond to the distances $r_{2j}=13, 469, 16\,897, \ldots$, and their scaling behavior can be obtained by the following analysis.

Consider a pair of neighboring effective spins belonging to the same block in the jth generation, and let c_0 be their zeroth-order correlation. Each of these spins represents 3^{j-1} real spins, so that for each such pair there are 3^{j-1} pairs of real spins separated by the same distance r_j, contributing to the total correlation per site $C(r_j)$. However, the contribution of a real pair to $C(r_j)$ depends on the string of Clebsch-Gordan coefficients indicating the weight of its two spins in the effective spins: each time the intermediate effective spin representing a real spin S_k is located at the ends (the center) of a three-spin block, the weight of S_k is multiplied by a factor $c_{1,3}$ ($c_{2,3}$) upon renormalization. (These coefficients are in general different for *xx* and *zz* correlations; see Appendix A.) Since each effective spin in the jth generation has gone through j-1 renormalizations, a real pair can be classified according to the number n of factors $c_{1,3}$ present in the (equal) weights of its spins. The contribution of all type-n pairs to $C(r_j)$ is proportional to the number of such pairs, being given by

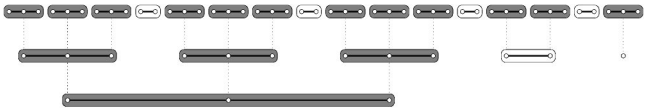

FIG. 11. First three generations of the *XXZ* chain with couplings following the sequence in Sec. V D, for $J_a < J_b$, showing an effective-spin hierarchy. Solid lines indicate strong bonds; for clarity, weak bonds are not represented. Shaded blocks contribute effective spins when renormalized, while white blocks form singlets. A third-generation effective spin represents three second-generation and nine first-generation spins.

$$g_j^{(n)} = 2^n \frac{(j-1)!}{n!(j-1-n)!} \left(c_{1,3}^2\right)^n \left(c_{2,3}^2\right)^{j-1-n} |c_0|.$$

Thus, the total contribution of a single effective-spin pair to $C(r_j)$ is

$$g_j = \sum_{n=0}^{j-1} g_j^{(n)} = (c_{2,3}^2 + 2c_{1,3}^2)^{j-1} |c_0|,$$

which gives

$$C(r_j) \sim n_j g_j \sim \frac{\left(c_{2,3}^2 + 2c_{1,3}^2\right)^j}{r_j},$$

where n_j is the fraction of active spins in the jth generation. Since asymptotically we have $j = \ln(r_j/r_0)/\ln\sqrt{\tau_{\rm bm}}$, this last result can be written as

$$C(r_j) \sim r_j^{-\eta}, \quad \text{with} \quad \eta = 1 - \frac{\ln\left(c_{2,3}^2 + 2c_{1,3}^2\right)}{\ln\sqrt{\tau_{\rm bm}}}. \qquad (18)$$

For the Heisenberg chain, $c_{1,3}=\gamma_3=\frac{2}{3}$ and $c_{2,3}=\frac{1}{3}$, so that $\eta=1$. For the *XX* chain, η depends on whether we look at longitudinal or transverse correlations; in the former case we have $c_{1,3}^{xx}=1/\sqrt{2}$ and $c_{2,3}^{xx}=\frac{1}{2}$, so that $\eta^{xx}\simeq 0.875$, while in the latter case $c_{1,3}^{zz}=\frac{1}{2}$, $c_{2,3}^{zz}=0$, and so $\eta^{zz}\simeq 1.387$. These values are fully compatible with the results from numerical implementations of the MDH scheme shown in Fig. 10, and they agree very well with free-fermion calculations for *XX* chains with $\rho \ll 1$. Again, larger coupling ratios lead to nonuniversal decay of the correlations, except in the Heisenberg limit.

D. A sequence producing effective-spin triples

The appearance of an effective-spin hierarchy is better illustrated by the sequence obtained from the substitution rule $a \to bbaba$, $b \to bba$. The first three generations of the chains, for $J_a < J_b$, are shown in Fig. 11; for $J_a > J_b$ the first lattice sweep interchanges the roles of weak and strong bonds, recovering the former case. Renormalization involves both three-spin and two-spin blocks, and each lattice sweep reproduces the original sequence, yielding effective couplings given by

$$J_a' = \gamma_2 \gamma_3^2 \frac{J_a^2}{J_b} \quad \text{and} \quad J_b' = \gamma_3^2 J_a,$$

so that the recursion relations for the coupling ratio and the energy gap are

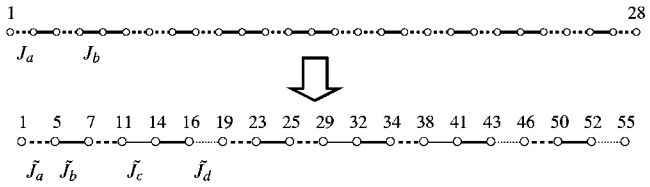

FIG. 12. First two generations of the *XXZ* chain with couplings following the sequence in Sec. V E, for $J_a < J_b$. The numbers indicate the position of the spins in the original chain. The first lattice sweep generates a fixed-point bond distribution with four different effective couplings $\tilde{J}_a$ through $\tilde{J}_d$.

$$\rho' = \gamma_2 \rho \quad \text{and} \quad \Lambda' = \gamma_3^2 \rho \Lambda.$$

The size of three-spin blocks follows $r_j = 2, 6, 22, \ldots$, while that of two-spin blocks corresponds to $r_j/2$, leading asymptotically to a rescaling factor

$$\tau_{\text{st}} = 2 + \sqrt{3} \simeq 3.73,$$

and a dynamical scaling relation

$$\Lambda_j \sim r_j^{-\zeta(\rho)} e^{-\mu \ln^2(r_j/r_0)},$$

with

$$\zeta(\rho) = -\frac{\ln(\gamma_2^{-1/2}\gamma_3^2\rho)}{\ln \tau_{\text{st}}} \quad \text{and} \quad \mu = -\frac{\ln(\gamma_2^{1/2})}{\ln^2 \tau_{\text{st}}}.$$

Again, aperiodicity induces nonuniversal behavior for $0 \leqslant \Delta < 1$ and a weakly exponential scaling in the Heisenberg limit.

As in the bronze-mean chains discussed in the previous Sec. V C, excitations of a given energy involve an exponentially large number of spins, due to the effective-spin hierarchy. More precisely, since each effective spin in the jth generation represents 3^{j-1} real spins, excitations with energy Λ_j, corresponding to breaking a jth generation singlet, involve $(2)3^{j-1}$ spins; exciting a three-spin block in the same generation costs an energy of the same order and involves 3^j spins. Dominant ground-state correlation functions also decay as in Eq. (18), but now with

$$\eta = 1 - \frac{\ln(c_{2,3}^2 + 2c_{1,3}^2)}{\ln \tau_{\text{st}}},$$

yielding $\eta^{xx} \simeq 0.830$ and $\eta^{zz} \simeq 1.526$ for the *XX* chain, and $\eta = 1$ for the Heisenberg chain. These values are again fully compatible with the results from numerical implementations of the MDH scheme.

E. A marginal tripling sequence

This sequence is generated by the substitution rule $a \to aba$, $b \to bba$. As discussed in Ref. 17, this type of aperiodicity may lead to marginal behavior even in anisotropic *XY* chains. As shown in Fig. 12, for $J_a < J_b$ the MDH scheme produces a second-generation lattice with four different effective couplings, given by

$$\tilde{J}_a = \gamma_2 \gamma_3 \frac{J_a^2}{J_b}, \quad \tilde{J}_b = \gamma_3 J_a,$$

$$\tilde{J}_c = \gamma_3^2 J_a, \quad \tilde{J}_d = \gamma_2 \frac{J_a^2}{J_b},$$

with an effective coupling ratio $\tilde{\rho} = \tilde{J}_a/\tilde{J}_b = \gamma_2 \rho$. (Choosing $J_a > J_b$ interchanges the roles of $\tilde{J}_c$ and $\tilde{J}_d$, otherwise producing the same bond distribution.) The bond distribution does not change upon further lattice sweeps, and the effective couplings satisfy the recursion relations

$$\tilde{J}_a' = \gamma_2 \frac{\tilde{J}_a^2}{\tilde{J}_b}, \quad \tilde{J}_b' = \gamma_2 \frac{\tilde{J}_c \tilde{J}_d}{\tilde{J}_b},$$

$$\tilde{J}_c' = \gamma_2 \frac{\tilde{J}_a \tilde{J}_c}{\tilde{J}_b}, \quad \tilde{J}_d' = \gamma_2 \frac{\tilde{J}_a \tilde{J}_d}{\tilde{J}_b}.$$

Noting that $\tilde{J}_a = \tilde{J}_c \tilde{J}_d / \tilde{J}_b$, we can write

$$\tilde{\rho}' = \frac{\tilde{J}_a'}{\tilde{J}_b'} = \frac{\tilde{J}_a}{\tilde{J}_b} = \tilde{\rho},$$

so that aperiodicity is marginal even in the Heisenberg limit. The recursion relation for the gaps is

$$\Lambda' = \frac{\tilde{J}_b'}{\tilde{J}_b} \Lambda = \gamma_2 \tilde{\rho} \Lambda,$$

and the size of the singlets formed along the generations follows $r_j = 3^j - 1$, with a rescaling factor $\tau_{\text{mt}} = 3$, so that the dynamic scaling relation is given by

$$\Lambda_j \sim r_j^{-\zeta(\rho)},$$

with a nonuniversal dynamical exponent

$$z = \zeta(\rho) = -\frac{\ln(\gamma_2^2 \rho)}{\ln 3}.$$

Thermodynamic properties can be estimated by using the same idea of the "independent-singlet" approximation described for Fibonacci chains, with slight modifications due to the fact that the first lattice sweep (but not the later ones) involves renormalization of both two- and three-spin blocks. Thus, the free energy per site can be calculated by adding to Eq. (13) a term representing the contribution of spins renormalized in the first lattice sweep, and given by

$$f_1(h,T) = \frac{1}{6} F_{\text{pair}}(J_b, \Delta_b; h, T) + \frac{1}{6} F_{\text{triple}}(J_b, \Delta_b; h, T), \quad (19)$$

where $F_{\text{triple}}(J, \Delta; h, T)$ is the free energy of a spin triple obeying the Hamiltonian

$$H_{\text{triple}} = J(S_1^x S_2^x + S_1^y S_2^y + \Delta S_1^z S_2^z) + J(S_2^x S_3^x + S_2^y S_3^y + \Delta S_2^z S_3^z) - h(S_1^z + S_2^z + S_3^z).$$

Notice that three-spin blocks yield effective spins when renormalized, and these will pair with other real or effective spins to form singlets in the second lattice sweep, but this is not taken into account by Eq. (19). In order to obtain a correct estimate of the low-temperature susceptibility, we must

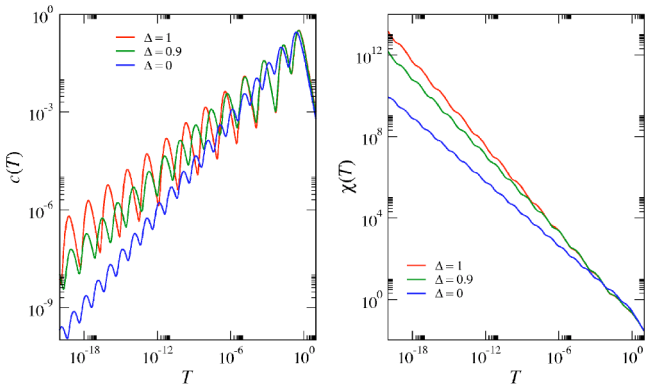

FIG. 13. (Color online) Log-log plots of the specific heat $c(T)$ and susceptibility $\chi(T)$ as functions of temperature for *XXZ* chains with couplings following the marginal tripling sequence, for $J_a/J_b = \frac{1}{10}$ and three different values of the uniform anisotropy Δ.

multiply the contribution arising from spin triples by a factor like $e^{-J_b/T}$. Results for the temperature dependence of the specific heat and susceptibility are shown in Fig. 13, for $\rho = \frac{1}{10}$ and three values of the uniform anisotropy Δ, corresponding to the *XX* and Heisenberg chains and to an intermediate case. Both quantities exhibit log-periodic oscillations, obeying the scaling forms

$$c(T) \sim T^{1/z} G_c\left(\frac{\ln T}{\ln \lambda}\right) \quad \text{and} \quad \chi(T) \sim T^{1/z-1} G_\chi\left(\frac{\ln T}{\ln \lambda}\right),$$

with λ being the asymptotic ratio between the gaps in successive generations, while G_c and G_χ are periodic functions (with a period of 1). In the *XX* and Heisenberg limits, we have $\lambda = \gamma_2^2 \rho$; for intermediate anisotropies, λ equals ρ_{eff}, a coupling ratio defined at the energy scale in which effective anisotropies become negligible.

Also as a consequence of the strictly marginal character of aperiodic fluctuations for all anisotropies in the regime $0 \leqslant \Delta \leqslant 1$, dominant ground-state correlations follow $C(r_j) \sim 1/r_j$ in the $\rho \ll 1$ regime, but nonuniversal behavior should be observed for larger coupling ratios.

VI. RELEVANT APERIODICITY

A. The binary Rudin-Shapiro sequence

The Rudin-Shapiro sequence is originally defined as a four-letter sequence,[56] generated by the substitution rule $a \to ac$, $b \to dc$, $c \to ab$, and $d \to db$. It has the interesting property that its geometrical fluctuations mimic those induced by a random distribution. In order to reduce it to a binary sequence, we make the associations $c \equiv a$ and $d \equiv b$, obtaining an inflation rule for letter pairs, given by $aa \to aaab$, $ab \to aaba$, $ba \to bbab$, and $bb \to bbba$. The rule generates blocks having between two and five spins and is symmetric under the interchange of a and b, so that the scaling behavior is invariant with respect to the interchange of J_a and J_b. The left end of the first two generations of the Rudin-Shapiro chains is shown in Fig. 14 for $J_a < J_b$.

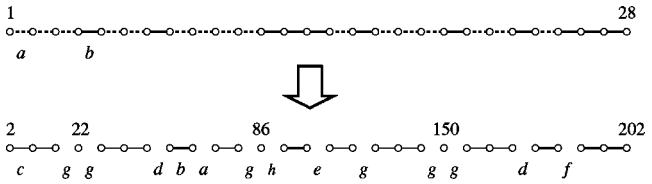

FIG. 14. First two generations of the binary Rudin-Shapiro *XXZ* chain, for $J_a < J_b$. The first lattice sweep generates eight different effective couplings, $\tilde{J}_a$ through $\tilde{J}_h$, labeled in the figure by the letters *a*–*h*. Further renormalization does not change the bond distribution. Starting from the second generation, only blocks coupled by $\tilde{J}_b$ (thick lines) and $\tilde{J}_c$ (thin lines) bonds are renormalized. (For clarity, weaker bonds are not drawn in the picture.)

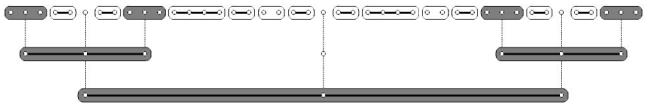

FIG. 15. Pattern of three-spin blocks and isolated spins leading to the effective-spin hierarchy in Rudin-Shapiro *XXZ* chains. Thick lines indicate strong bonds. Shaded blocks contribute effective spins when renormalized; white blocks form singlets.

Blocks with more than three spins are eliminated in the first lattice sweep and do not appear in later generations. Both two- and three-spin blocks are present in the fixed-point block distribution (already reached at the second generation), and upon renormalization the sequence produces an effective-spin hierarchy, stemming from approximately mirror-symmetric patterns of three-spin and five-spin blocks in the original lattice. This is illustrated in Figs. 15 and 16.

In the jth generation, three-spin blocks have size $r_j = (2)4^{j-1}$ (with a rescaling factor $\tau_{\text{rs}} = 4$), while two-spin blocks have size $r_j/2$. The first lattice sweep generates effective couplings $\tilde{J}_i$ having eight different values,

$$\tilde{J}_a = \gamma_2 \gamma_3 \gamma_4 \frac{J_a^5}{J_b^4}, \quad \tilde{J}_b = \gamma_3 \gamma_5 J_a,$$

$$\tilde{J}_c = \gamma_2 \gamma_3 \frac{J_a^2}{J_b}, \quad \tilde{J}_d = \gamma_3 \gamma_4 \gamma_5 \frac{J_a^2}{J_b}, \quad \tilde{J}_e = \gamma_2^2 \gamma_3 \gamma_5 \frac{J_a^2}{J_b},$$

$$\tilde{J}_f = \gamma_2^2 \gamma_3 \gamma_4 \gamma_5 \frac{J_a^3}{J_b^2}, \quad \tilde{J}_g = \gamma_2^2 \gamma_3 \gamma_4 \frac{J_a^4}{J_b^3}, \quad \tilde{J}_h = \gamma_2^3 \gamma_3 \gamma_4^2 \frac{J_a^5}{J_b^4},$$

and whose bond distribution remains unchanged upon renormalization, leading to the recursion relations

$$\tilde{J}_a' = \gamma_2^3 \frac{\tilde{J}_a^2 \tilde{J}_d \tilde{J}_g}{\tilde{J}_b \tilde{J}_c^2}, \quad \tilde{J}_b' = \gamma_3 \tilde{J}_f,$$

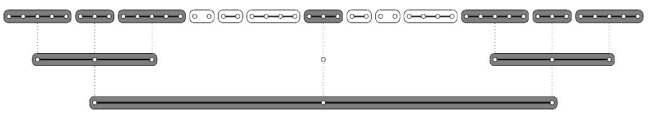

FIG. 16. Pattern of five-spin and three-spin blocks leading to the effective-spin hierarchy in Rudin-Shapiro *XXZ* chains. Thick lines indicate strong bonds. Shaded blocks contribute effective spins when renormalized; white blocks form singlets.

$$\tilde{J}_c' = \gamma_3 \tilde{J}_g, \quad \tilde{J}_d' = \gamma_2 \gamma_3^2 \frac{\tilde{J}_d \tilde{J}_f}{\tilde{J}_b}, \quad \tilde{J}_e' = \gamma_2 \gamma_3^2 \frac{\tilde{J}_e \tilde{J}_g}{\tilde{J}_c},$$

$$\tilde{J}_f' = \gamma_2^2 \gamma_3 \frac{\tilde{J}_a \tilde{J}_d \tilde{J}_f}{\tilde{J}_b \tilde{J}_c^2}, \quad \tilde{J}_g' = \gamma_2^2 \gamma_3 \frac{\tilde{J}_a \tilde{J}_d \tilde{J}_g}{\tilde{J}_b \tilde{J}_c}, \quad \tilde{J}_h' = \gamma_2^3 \frac{\tilde{J}_e \tilde{J}_f \tilde{J}_h^2}{\tilde{J}_b^2 \tilde{J}_c}.$$

Defining a new effective coupling $\tilde{J}_0 = \tilde{J}_a \tilde{J}_d / \tilde{J}_c$, we obtain a system of three recursion relations,

$$\tilde{J}_0' = \gamma_2^4 \gamma_3 \frac{\tilde{J}_0^2 \tilde{J}_f}{\tilde{J}_b^2}, \quad \tilde{J}_b' = \gamma_3 \tilde{J}_f, \quad \text{and} \quad \tilde{J}_f' = \gamma_2^2 \gamma_3 \frac{\tilde{J}_0 \tilde{J}_f}{\tilde{J}_b}.$$

With coupling ratios $\tilde{\rho} = \tilde{J}_0 / \tilde{J}_b$ and $\tilde{\sigma} = \tilde{J}_f / \tilde{J}_b$, and a gap proportional to $\tilde{J}_b$, we have

$$\tilde{\rho}_j = \gamma_2^4 \tilde{\rho}_{j-1}^2, \quad \tilde{\sigma}_j = \gamma_2^2 \tilde{\rho}_{j-1}, \quad \text{and} \quad \frac{\Lambda_j}{\Lambda_{j-1}} = \gamma_3 \tilde{\sigma}_j,$$

which, after eliminating $\tilde{\sigma}_j$, yields

$$\tilde{\rho}_j = \gamma_2^4 \tilde{\rho}_{j-1}^2 \quad \text{and} \quad \frac{\Lambda_j}{\Lambda_{j-1}} = \gamma_3 \tilde{\rho}_j^{1/2}.$$

Solving the recursion relations we obtain

$$\Lambda_j \sim r_j^{-\zeta} \exp\left[-\mu \left(\frac{r}{r_0} \right)^{\omega} \right]$$

with $\omega = \frac{1}{2}$,

$$\zeta = \frac{\ln(\gamma_3 / \gamma_2^2)}{\ln \tau_{\rm rs}} \quad \text{and} \quad \mu = -\frac{1}{2} \ln(\gamma_2^2 \gamma_4 \rho^2).$$

So we obtain, for the whole regime $0 \leqslant \Delta \leqslant 1$, the dynamical scaling form predicted for the *XX* chain, reproducing the result for the random-singlet phase.

For chains with RS couplings, effective-spin formation determines the dominant ground-state correlations, but the corresponding hierarchy is slightly different from the ones seen in Secs. V C and V D, now involving both three-spin (and some five-spin) blocks and unrenormalized spins. As illustrated in Figs. 15 and 16, for each block renormalized in the jth generation the correlation between its end spins connects a number of order 2^j original spin pairs separated by the same distance r_j (the size of the block), yielding a contribution to the average correlation in the Heisenberg chain and $C^{xx}(r_j)$ in the *XX* chain given by

$$g_j = \left[(2c_{1,3}^2)^{j-1} + c_{2,3}^2 \sum_{k=1}^{j-1} (2c_{1,3}^2)^{k-1} \right] |c_0|,$$

where c_0 is the correlation between end spins in a three-spin block. For the Heisenberg chain $2c_{1,3}^2 = \frac{8}{9} < 1$, and thus,

$$C(r_j) \sim g_j n_j \sim \frac{1}{r_j}, \tag{20}$$

where $n_j \sim 1/r_j$ is the fraction of three-spin blocks in the jth generation. For the *XX* chain $2(c_{1,3}^{xx})^2 = 1$, so that g_j has a term proportional to j, and $C^{xx}(r_j)$ carries a logarithmic correction,

$$C^{xx}(r_j) \sim g_j n_j \sim (y_0 + y_1 \ln r_j) r_j^{-1}, \tag{21}$$

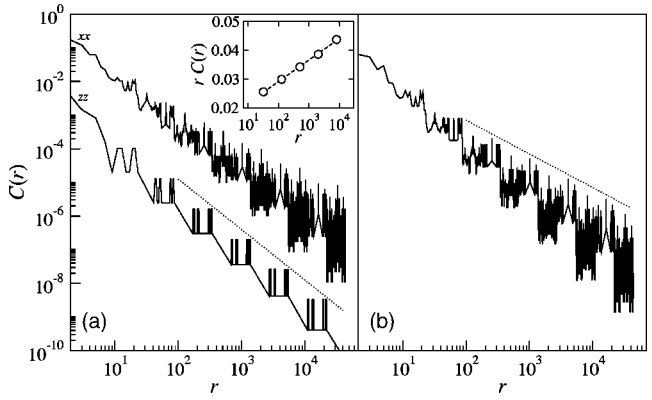

FIG. 17. Ground-state correlations for chains with Rudin-Shapiro couplings, obtained from extrapolation of numerical MDH results for chains with 2^{16} to 2^{20} sites. (a) $C^{xx}(r)$ (upper solid curve) and $C^{zz}(r)$ (lower solid curve) for the *XX* chain. The dotted curve is proportional to $r^{-3/2}$. (Curves offset for clarity.) Inset: dominant C^{xx} correlations, corresponding to distances $r_j = (2)4^{j-1}$, fitted by a law of the form $rC^{xx}(r) = y_0 + y_1 \ln r$ (dashed curve). (b) $C(r)$ for the Heisenberg chain (solid curve). The dotted curve is proportional to $1/r$.

where y_0 and y_1 are constants. The *zz* correlation between end spins in a three-spin block is zero, so that the dominant correlations correspond to spin pairs (connected through one of the effective end spins and the middle spin) at distances $r_j' = 4^{j-1} \pm 4^{j-2} \pm 4^{j-3} \pm \cdots \pm 1$, with average $\langle r_j' \rangle = 4^{j-1}$, whose contribution is given by $g_j' \sim (\frac{1}{2})^{j-1}$, since $c_{1,3}^{zz} = \frac{1}{2}$. We then have

$$C^{zz}(r_j') \sim g_j' n_j \sim \langle r_j' \rangle^{-3/2}. \tag{22}$$

Eqs. (21) and (22) should be contrasted with the random-singlet isotropic result $C(r) \sim r^{-2}$, indicating a clear distinction between the ground-state phases induced by disorder and aperiodicity, even in the presence of similar geometric fluctuations. This is related to the inflation symmetry of the aperiodic sequences, which is absent in the random-bond case (or in aperiodic systems with random perturbations[57]). Its effects are exemplified by the fractal structure of the ground-state correlations visible in Fig. 17, which displays results from numerical implementations of the MDH method for both *XX* and Heisenberg chains, showing conformance to the scaling forms in Eqs. (20)–(22). Contrary to the marginal sequences, these scaling forms should be observed in the large-distance behavior of Rudin-Shapiro *XXZ* chains for any coupling ratio $\rho \neq 1$; we expect a crossover from the uniform to aperiodic scaling behavior as larger distances are probed for ρ close to unity. Free-fermion calculations in the *XX* limit support this picture.

B. The 6-3 sequence

This sequence is generated by the substitution $a \rightarrow babaaa$, $b \rightarrow baa$, and its *XX* wandering exponent is $\omega = \ln 2 / \ln 5$, with a rescaling factor $\tau_{63} = 5$. Application of the MDH scheme leads to a fixed-point bond distribution with singlet renormalization only, so that no effective-spin hierar-

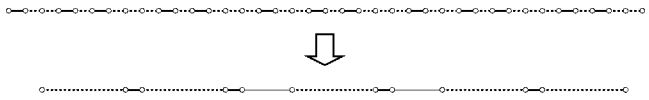

FIG. 18. First two generations of the 6-3 sequence, discussed in Sec. VI B, for $J_a < J_b$. In the second generation, dashed lines indicate effective $\tilde{J}_a$ bonds, while thick and thin solid lines denote effective $\tilde{J}_b$ and $\tilde{J}_c$ bonds. In subsequent generations, the $\tilde{J}_c\tilde{J}_a$ pairs change to $\tilde{J}_a\tilde{J}_c$, and the first $\tilde{J}_a$ becomes $\tilde{J}_c$, but the bond distribution is otherwise unchanged.

chy is present. For $J_a < J_b$, as depicted in Fig. 18, three effective couplings are produced after the first lattice sweep,

$$\tilde{J}_a = \gamma_2^2 \frac{J_a^3}{J_b^2}, \quad \tilde{J}_b = J_a, \quad \tilde{J}_c = \gamma_2 \frac{J_a^2}{J_b},$$

and upon further lattice sweeps we obtain the recursion relations

$$\tilde{J}_a' = \gamma_2^3 \frac{\tilde{J}_a^3 \tilde{J}_c}{\tilde{J}_b^3}, \quad \tilde{J}_b' = \gamma_2 \frac{\tilde{J}_a \tilde{J}_c}{\tilde{J}_b}, \quad \tilde{J}_c' = \gamma_2^2 \frac{\tilde{J}_a^2 \tilde{J}_c}{\tilde{J}_b^2}.$$

Thus, defining the effective coupling ratios

$$\tilde{\rho} \equiv \frac{\tilde{J}_a}{\tilde{J}_b} = \gamma_2^2 \left(\frac{J_a}{J_b}\right)^2 \quad \text{and} \quad \tilde{\sigma} = \frac{\tilde{J}_c}{\tilde{J}_b} = \gamma_2 \frac{J_a}{J_b},$$

we can rewrite the recursion relations as

$$\tilde{\rho}' = \gamma_2^2 \tilde{\rho}^2, \quad \tilde{\sigma}' = \gamma_2 \tilde{\rho}, \quad \text{and} \quad \frac{\Lambda'}{\Lambda} = \frac{\tilde{J}_b'}{\tilde{J}_b} = \gamma_2 \tilde{\sigma} \tilde{\rho}.$$

In the jth generation, we have $\tilde{\sigma}_j^2 = \tilde{\rho}_j$, and thus,

$$\tilde{\rho}_{j+1} = \gamma_2^2 \tilde{\rho}_j^2 \quad \text{and} \quad \Lambda_{j+1} = \gamma_2 \tilde{\rho}_j^{3/2} \Lambda_j.$$

The length of the singlets correspond to $r_j = 1, 9, 45, 225, \ldots$, so that asymptotically $r_j \sim r_0 \tau^j$, with $r_0 = \frac{9}{25}$ and $\tau = \tau_{63} = 5$. Solving the above recursion relations we obtain the dynamical scaling behavior,

$$\Lambda_j \sim r_j^{-\zeta} \exp\left[-\mu \left(\frac{r}{r_0}\right)^{\omega} \right], \tag{23}$$

with a wandering exponent $\omega = \ln 2 / \ln 5 \simeq 0.431$ and

$$\zeta = \frac{3 \ln \gamma_2}{\ln 5} \quad \text{and} \quad \mu = -\frac{3}{2} \ln(\gamma_2^4 \rho^3),$$

where $\rho = J_a / J_b$ is the original coupling ratio.

If we choose $J_a > J_b$, blocks with 2, 3, and 4 spins coupled by strong bonds appear along the chain. Effective spins are produced by the first lattice sweep, yielding effective couplings

$$\tilde{J}_a = \gamma_2^3 \gamma_3^2 \gamma_4^3 \frac{J_b^7}{J_a^6}, \quad \tilde{J}_b = \gamma_2 \gamma_3^2 \gamma_4 \frac{J_b^3}{J_a^2}, \quad \text{and} \quad \tilde{J}_c = \gamma_2^2 \gamma_3^2 \gamma_4^2 \frac{J_b^5}{J_a^4},$$

whose distribution is the same as that of the third-generation bonds for $J_a < J_b$, and which remains unchanged upon renormalization. Thus, the scaling behavior is the same as above, but now with a bare coupling ratio

$$\tilde{\rho} \equiv \frac{\tilde{J}_a}{\tilde{J}_b} = \gamma_2^2 \gamma_4^2 \left(\frac{J_b}{J_a}\right)^4.$$

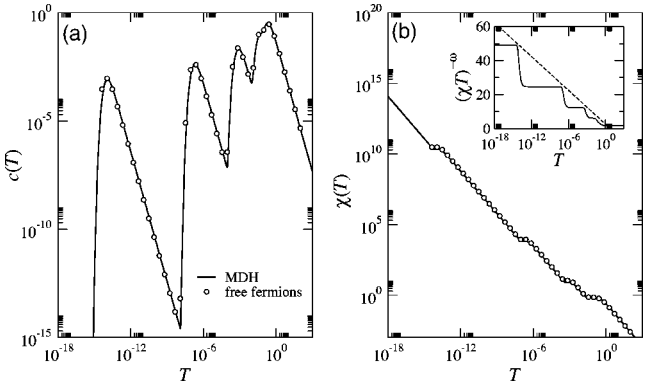

FIG. 19. Thermal dependence of the specific heat (a) and susceptibility (b) of the *XX* chain with couplings following the 6-3 sequence of Sec. VI B, obtained for $J_a/J_b = \frac{1}{4}$ from both numerical diagonalization of chains with 46 875 sites (circles) and the MDH scheme (solid curves). The inset in (b) presents a log-linear plot of T versus $(\chi T)^{-\omega}$, with $\omega = \ln 2 / \ln 5$, showing that for $T \simeq \Lambda_j$, corresponding to the specific-heat maxima, the susceptibility satisfies the scaling form $\chi \sim T^{-1} |\ln T|^{-1/\omega}$ (dashed line); at intermediate temperatures, a Curie-like behavior is observed.

Thermodynamic properties can be estimated as in the Fibonacci case, by using the independent-singlet approximation. Plots of the specific heat $c(T)$ and susceptibility $\chi(T)$ as functions of temperature are shown in Fig. 19, and compare quite well with results from numerical diagonalization, even for relatively large coupling ratios $(J_a/J_b = \frac{1}{4})$. This is not surprising, given the fact that the effective coupling ratio rapidly decreases as the RG proceeds, even for the *XX* chain. As seen in the inset of Fig. 19(b), at temperatures of the order of the gaps Λ_j the susceptibility follows the scaling form

$$\chi(T) \sim \frac{1}{T |\ln T|^{1/\omega}},$$

which can be readily obtained from Eq. (23) by assuming that singlet pairs are magnetically frozen, while active spins contribute Curie terms to χ. Estimates of $c(T)$ and $\chi(T)$ for chains with anisotropies $0 < \Delta \leqslant 1$ are qualitatively identical to the ones for the *XX* chain.

Since no effective-spin hierarchy is present, and aperiodicity is relevant, dominant ground-state correlations, for any coupling ratio $\rho \neq 1$ and sufficiently large characteristic distances r_j, should decay as

$$C^{xx}(r_j) \sim C^{zz}(r_j) \sim \frac{1}{r_j},$$

for all anisotropies in the regime $0 \leqslant \Delta \leqslant 1$. This is confirmed in the *XX* limit by numerical diagonalization, as shown in Fig. 20.

C. The fivefold-symmetry sequence

The sequence produced by the substitution rule $a \to aaab$, $b \to bba$ is related to binary tilings of the plane with fivefold symmetry.[36] The (quite large) *XX* rescaling factor is $\tau_{\rm ff}=25+10\sqrt{5}\simeq 47.36$, with a wandering exponent $\omega = \ln 3/\ln \tau_{\rm ff}\simeq 0.285$.

Under a numerical implementation of the MDH scheme with $J_a<J_b$, we obtain a quite intricate pattern. After a four-bond transient produced by the first two lattice sweeps, a two-cycle periodic attractor is reached, where six- and seven-bond distributions alternate, as depicted in Fig. 21. (With $J_a>J_b$, the same two-cycle is reached after the first lattice sweep.) The distance between spins connected by the strongest bonds in each generation correspond to $r_j = 1,3,33,190,1385,9050,\ldots$, which asymptotically gives $r_{j+2}/r_j \simeq \tau_{\rm ff}$. The equations relating the effective couplings of the fourth and fifth generations are

$$\tilde{J}_a = \gamma_2^3\gamma_3\frac{\tilde{J}_A^2\tilde{J}_C\tilde{J}_F}{\tilde{J}_B^3}, \quad \tilde{J}_b = \gamma_3\tilde{J}_E, \quad \tilde{J}_c = \gamma_2^2\frac{\tilde{J}_A\tilde{J}_C\tilde{J}_G}{\tilde{J}_B^2},$$

$$\tilde{J}_d = \gamma_2^2\frac{\tilde{J}_C\tilde{J}_E\tilde{J}_F}{\tilde{J}_B\tilde{J}_D}, \quad \tilde{J}_e = \gamma_3^2\frac{\tilde{J}_A^2\tilde{J}_C\tilde{J}_G}{\tilde{J}_B^3}, \quad \tilde{J}_f = \gamma_2^2\gamma_3\frac{\tilde{J}_A\tilde{J}_C\tilde{J}_F}{\tilde{J}_B^2},$$

while between the couplings of the fifth and fourth generations we have

$$\tilde{J}'_A = \gamma_2^2\gamma_3\frac{\tilde{J}_e^2\tilde{J}_f}{\tilde{J}_b\tilde{J}_c}, \quad \tilde{J}'_B = \gamma_2\gamma_3\frac{\tilde{J}_d\tilde{J}_f}{\tilde{J}_b}, \quad \tilde{J}'_C = \gamma_2\frac{\tilde{J}_e\tilde{J}_f}{\tilde{J}_b},$$

$$\tilde{J}'_D = \gamma_2^6\gamma_3^2\frac{\tilde{J}_a^2\tilde{J}_d\tilde{J}_e\tilde{J}_f}{\tilde{J}_b^3\tilde{J}_c}, \quad \tilde{J}'_E = \gamma_2^6\gamma_3\frac{\tilde{J}_a^2\tilde{J}_e^2\tilde{J}_f}{\tilde{J}_b^3\tilde{J}_c},$$

$$\tilde{J}'_F = \gamma_2^8\gamma_3^2\frac{\tilde{J}_a^3\tilde{J}_d\tilde{J}_e\tilde{J}_f}{\tilde{J}_b^4\tilde{J}_c}, \quad \tilde{J}'_G = \gamma_2^8\gamma_3\frac{\tilde{J}_a^3\tilde{J}_e^2\tilde{J}_f}{\tilde{J}_b^4\tilde{J}_c}.$$

Eliminating the fifth-generation couplings and defining the ratios

$$\tilde{\rho} = \frac{\tilde{J}_A}{\tilde{J}_B}, \quad \sigma_1 = \frac{\tilde{J}_C}{\tilde{J}_B}, \quad \sigma_2 = \frac{\tilde{J}_F^2}{\tilde{J}_A\tilde{J}_B}, \quad \text{and} \quad \sigma_3 = \frac{\tilde{J}_F}{\tilde{J}_E},$$

we can write a set of four recursion relations,

$$\tilde{\rho}' = \gamma_2^3\tilde{\rho}_j^3, \quad \sigma'_1 = \frac{\gamma_2}{\gamma_3}\tilde{\rho}^2,$$

$$\sigma'_2 = \gamma_2^{22}\gamma_3\tilde{\rho}^9(\sigma_1\sigma_3)^4, \quad \sigma'_3 = \gamma_2^4\gamma_3\sigma_1\sigma_3.$$

The gaps in successive even generations obey

$$\frac{\Lambda'}{\Lambda} = \frac{\tilde{J}'_B}{\tilde{J}_B} = \gamma_2^5\gamma_3\rho\sigma_1^2\sigma_2,$$

and by expressing σ_1, σ_2, and σ_3 in terms of $\tilde{\rho}$ we get

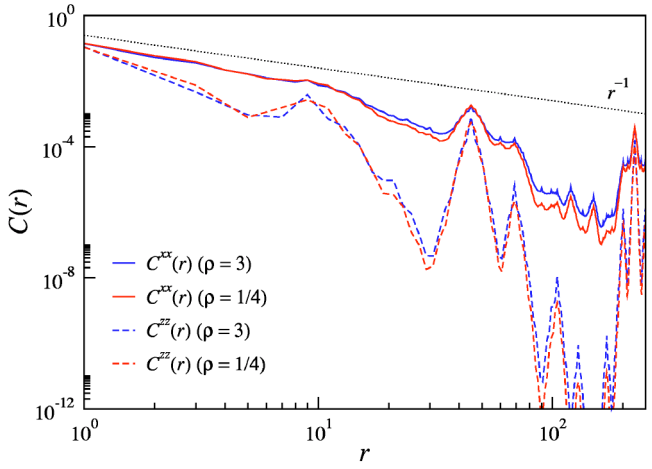

FIG. 20. (Color online) Ground-state correlations of the *XX* chain with couplings following the 6-3 sequence of Sec. VI B, for two different values of the coupling ratio $\rho=J_a/J_b$, as obtained by numerical diagonalization of chains with 1874 sites. Peaks in the curves correspond to the characteristic distances $r_j=9$, 45, and 225.

$$\frac{\Lambda_{j+1}}{\Lambda_j} = a\gamma_2^{20j}\tilde{\rho}_j^{16/3},$$

where now $2j+2$ labels the lattice generation and a is a constant, depending on the values of the coupling ratios in the fourth generation. Solving this last equation gives

$$\Lambda_j \sim A^j B^{j^2} C^{3^j},$$

with

$$A = a\gamma_2^{-8}, \quad B = \gamma_2^{20}, \quad \text{and} \quad C = \gamma_2^{4/9}\tilde{\rho}_1^{8/9}.$$

For large enough j, since $j=\ln(r_j/r_0)/\ln\tau_{\rm ff}$, we have

$$\Lambda_j \sim \exp\left[-\mu\left(\frac{r_j}{r_0}\right)^{\omega}\right],$$

with

$$\mu = -\ln C \quad \text{and} \quad \omega = \frac{\ln 3}{\ln \tau_{\rm ff}},$$

again obtaining, for the whole anisotropy regime $0\leqslant\Delta\leqslant 1$, the same scaling form predicted for the *XX* chain.

The effective-spin hierarchy produced by the RG process is analogous to that in the bronze-mean chains, so that ground-state correlations behave as in Eq. (18), with $\eta=1$ in the Heisenberg chain, but $\eta^{xx}\simeq 0.884$ and $\eta^{zz}\simeq 1.359$ in the *XX* limit. However, these figures are not so well reproduced in the numerical calculations, even for chains with $N\simeq 1.6\times 10^6$ sites, most probably due to the extremely large rescaling factor.

VII. DISCUSSION AND CONCLUSIONS

For all aperiodic sequences discussed in the previous sections, the recursion relations for the main coupling ratio and the energy gaps have the forms

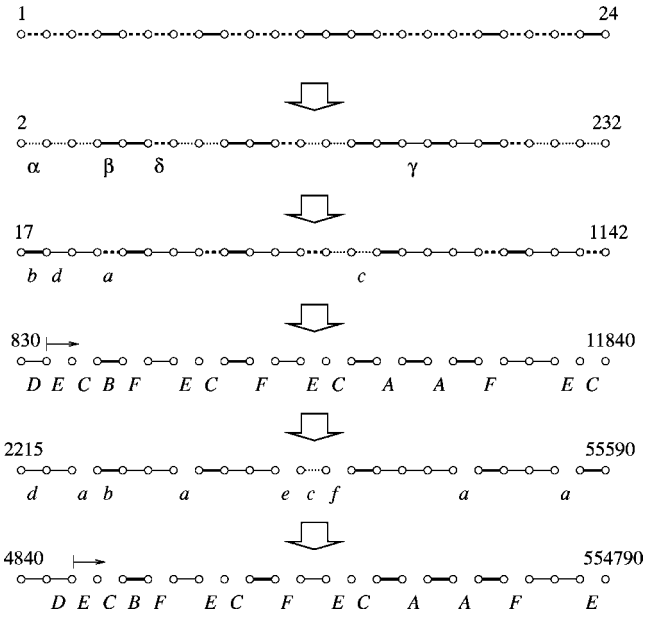

FIG. 21. Leftmost 24 sites in the first six generations of *XXZ* chains with couplings following the fivefold-symmetry sequence, discussed in Sec. VI C, for $J_a < J_b$. The attractor of the bond distribution is a two-cycle, reached after three lattice sweeps. Second-generation bonds are denoted by J_α through J_δ; third- and fifth-generation couplings are labeled *a* through *f*, while *A* through *G* label fourth- and sixth-generation bonds. Couplings J_G only occur much farther along the chains. Starting from the fourth generation, lines indicate blocks to be renormalized.

$$\rho_{j+1} = c\rho_j^k \quad \text{and} \quad \Lambda_{j+1} = f_1 f_2^j \rho_j^\ell \Lambda_j, \tag{24}$$

where c, f_1, and f_2 are Δ-dependent nonuniversal constants, and ℓ (a rational number) and k (an integer) relate to the number of singlets involved in determining the effective couplings. In particular, k is ultimately the difference in the number of singlets producing the effective couplings whose ratio is $\rho < 1$.

If $k \geqslant 2$, the recursion relation for ρ always has a stable fixed point at $\rho^* = 0$, so that the effective coupling ratios become exponentially small as the renormalization proceeds, indicating that asymptotic results obtained from the MDH method should be essentially exact. Taking into account the scaling behavior of the characteristic distances $r_j \sim r_0 \tau^j$, Eqs. (24) lead to the dynamical scaling form

$$\Lambda_j \sim r_j^{-\zeta} e^{-\mu' \ln^2(r_j/r_0)} e^{-\mu(r_j/r_0)^\omega} \sim e^{-\mu(r_j/r_0)^\omega}, \tag{25}$$

with ζ and μ' nonuniversal constants,

$$\mu = -\frac{\ln\left(c^{\ell/k-1}\rho^\ell\right)}{k(k-1)},$$

ρ being the bare coupling ratio, and

$$\omega = \frac{\ln k}{\ln \tau}.$$

Note that ω has the same form as the exact wandering exponent for *XX* chains with nondimerizing aperiodic couplings, given in Eq. (7). Moreover, ω depends only on the topology and the self-similar properties of the sequence, being independent of the anisotropy in the regime $0 \leqslant \Delta \leqslant 1$.

If $k=1$, the recursion relation for ρ has a line of fixed points, provided that $c=1$, which is generically the case in the *XX* limit; otherwise $\rho^*=0$ is a stable fixed point. The general solution to Eqs. (24) is

$$\Lambda_j \sim r_j^{-\zeta(\rho)} e^{-\mu \ln^2(r_j/r_0)}, \tag{26}$$

where

$$\zeta(\rho) = -\frac{\ln\left(f_1 f_2^{1/2} c^{-\ell/2} \rho^\ell\right)}{\ln \tau} \quad \text{and} \quad \mu = -\frac{\ln\left(f_2^{1/2} c^{\ell/2}\right)}{\ln^2 \tau}.$$

Unless $f_2 \neq 1$, which, among the sequences studied here, happens only for the relevant fivefold-symmetry sequence of Sec. VI C, μ is zero in the *XX* limit. This means that we can identify a nonuniversal dynamical exponent $z = \zeta(\rho)$, and the scaling behavior of thermodynamic properties depends on the coupling ratio for the whole anisotropy regime $0 \leqslant \Delta < 1$. In the Heisenberg limit ($\Delta = 1$), unless $\mu = 0$, as in the marginal tripling sequence of Sec. V E, Eq. (26) describes a weakly exponential dynamic scaling. In this case, aperiodicity can be viewed as a marginally relevant operator ($\omega \to 0^+$) in the renormalization-group sense.

These results strongly suggest that low-temperature thermodynamic properties of any antiferromagnetic *XXZ* chain with anisotropies intermediate between the *XX* and Heisenberg limits and couplings following a given binary aperiodic sequence can be classified according to a single wandering exponent ω, which is known exactly for *XX* chains. This generalizes what happens in random-bond *XXZ* chains (for which $\omega = \frac{1}{2}$), where thermodynamic properties in the anisotropy regime $-\frac{1}{2} \leqslant \Delta \leqslant 1$ are those characterizing the random-singlet phase.[8,43] Note that, although the above classification seems to imply an anisotropy-independent critical value $\omega_c = 0$ for the relevance of aperiodic fluctuations on the low-temperature behavior of *XXZ* chains, it does not show that ω plays the role of a genuine wandering exponent, in the sense that fluctuations scale as $g \sim N^\omega$ for general easy-plane anisotropies. In any case, due to the fact that the critical exponents (including the correlation-length exponent ν) of the uniform *XXZ* chain are known to vary with the anisotropy along the whole critical line $-1 \leqslant \Delta \leqslant 1$,[21,22] it remains an open question how the present results fit into the framework of the Harris-Luck criterion.

Of course, Eqs. (24) are valid for all anisotropies $0 \leqslant \Delta \leqslant 1$ only if the bond distribution generated by the MDH method is independent of Δ. This is certainly the case for strong enough modulation. (How strong this modulation has to be depends on the various block sizes produced by the sequence.) However, from numerical implementations of the method, we find that, even when the blocks selected for renormalization in the first few lattice sweeps depend on Δ, a universal distribution is eventually reached, in much the same way as when we choose $J_a > J_b$ instead of $J_a < J_b$. Thus, we expect that, for general binary substitution rules inducing relevant aperiodicity, the scaling form in Eq. (25) holds for all coupling ratios $\rho \neq 1$.

An approximate picture of the ground state and of the lowest excitations in the presence of aperiodic couplings can also be deduced from the MDH scheme, and is revealed by the behavior of the pair correlation functions. As the energy scale is reduced, two types of behavior can be identified. Either the RG process produces a hierarchy of singlets (as in the Fibonacci, silver-mean, marginal-tripling, and 6-3 sequences), or a hierarchy of effective spins (as in the bronze-mean, spin-triple, Rudin-Shapiro, and fivefold-symmetry sequences). The first type reveals a kind of self-similar, aperiodic-singlet phase, from which (singlet-triplet) excitations involve strongly coupled pairs composed of spins separated by well defined characteristic distances. In the second type, since the number of spins contributing to an effective spin increases exponentially along the hierarchy, excitations of a certain energy involve spins separated by a wide range of distances, giving rise to a fractal structure of the correlation functions. Notice that, contrary to the finite temperature behavior, there is no relation between the ground-state properties and the marginal or relevant character of the aperiodicity.

For aperiodic sequences inducing strictly marginal fluctuations, we could account for the nonuniversality of the correlation-function decay exponents by a numerical calculation based on a second-order expansion of the ground-state vectors. This compares quite well with results from numerical diagonalization in the *XX* limit, which indeed show that the zeroth-order MDH predictions are reproduced in the strong-modulation regime.

The results on relevant aperiodic couplings show that geometrical fluctuations, measured by the wandering exponent ω, are not determinant for ground-state properties, although they control the low-energy scaling of thermodynamic quantities. In particular, both random bonds and Rudin-Shapiro couplings are characterized by $\omega=\frac{1}{2}$; however, correlations in the random-singlet phase are entirely different from those in *XXZ* chains with Rudin-Shapiro couplings. This is a consequence of the inflation symmetry induced by substitution rules, which is clearly absent in random chains. (Analogously, comparative studies[58,59] between random-bond and Rudin-Shapiro quantum Ising chains show that, although the corresponding scaling properties are similar at the critical point, only randomness is capable of producing the off-critical Griffiths singularities.[1,2,60]) Nevertheless, aperiodic and random *XXZ* chains share the feature that the average and typical behaviors are strikingly distinct, and that average correlations decay as power laws. Finally, aperiodic ground-state phases are unstable towards random perturbations, which break inflation symmetry, and the random-singlet behavior is ultimately recovered.[57]

ACKNOWLEDGMENTS

This work has been supported by the Brazilian agencies CAPES and FAPESP. The author is indebted to T. A. S. Haddad, E. Miranda, J. A. Hoyos, A. P. S. de Moura, F. C. Alcaraz, and S. R. Salinas for helpful conversations.

APPENDIX A: RENORMALIZATION OF MULTI-SPIN BLOCKS

In this appendix, we derive the expressions for the renormalized coupling constants used in the extension of the Ma-

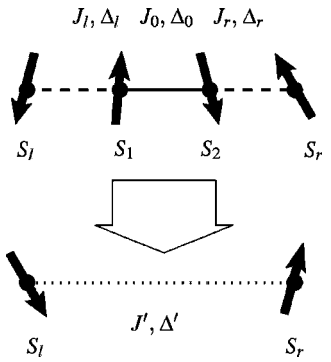

FIG. 22. Renormalization step involving the decimation of a two-spin block.

Dasgupta-Hu method to *XXZ* chains with aperiodic couplings. Contrary to the random-bond chains discussed in Sec. II, when couplings follow aperiodic sequences generated by inflation rules we generally need to consider spin blocks with more than one strong bond, and thus more than two spins. For instance, in the Fibonacci sequence with $J_a > J_b$ (see Fig. 2) there appear blocks with one or two J_a bonds. Since we assume that all couplings are antiferromagnetic, the local ground state is a singlet for blocks with an even number of spins, but a doublet if the blocks contain an odd number of spins.[61]

Let us consider a block with n spins S_1 through S_n connected by equal bonds J_0, with anisotropy Δ_0. This is described by the local Hamiltonian

$$H_0 = J_0 \sum_{j=1}^{n-1} (\mathbf{S}_j \cdot \mathbf{S}_{j+1})_{\Delta_0},$$

where we introduced the notation

$$(\mathbf{S}_i \cdot \mathbf{S}_j)_\Delta \equiv S_i^x S_j^x + S_i^y S_j^y + \Delta S_i^z S_j^z.$$

The gap Λ_0 between the ground-state energy of the block and its lowest excited multiplet depends on J_0 and Δ_0. For two-spin and three-spin blocks we have

$$\Lambda_0^{(2)} = \frac{1+\Delta_0}{2} J_0 \quad \text{and} \quad \Lambda_0^{(3)} = \frac{1}{4}\left(\Delta_0 + \sqrt{\Delta_0^2 + 8}\right) J_0.$$

We define the strongest bonds in the chain as those producing spin blocks with the largest gaps Λ_0.

An n-spin block to be renormalized is connected to its neighboring spins S_l and S_r by weaker bonds J_l and J_r. The relevant part of the chain Hamiltonian is

$$H = H_0 + H_{lr},$$

with

$$H_{lr} = J_l (\mathbf{S}_l \cdot \mathbf{S}_1)_{\Delta_l} + J_r (\mathbf{S}_n \cdot \mathbf{S}_r)_{\Delta_r}. \tag{A1}$$

The idea of the MDH method is to obtain recursion relations for the couplings by treating H_{lr} as a perturbation to H_0.

If n is even (as in the two-spin case shown in Fig. 22), the ground state of H_0 is a singlet, which we denote by $|\Psi_0\rangle$, with a corresponding energy E_0. In the space of this singlet, the states of S_l and S_r are arbitrary. In the space spanned by

the eigenstates $|\Psi_i\rangle$ of H_0 (with energies E_i) and the states $|m_l,m_r\rangle \equiv |m_l\rangle \otimes |m_r\rangle$ of $S_{l,r}$ $\left(m_{l,r}=\pm\frac{1}{2}\right)$, the states $|g(m_l,m_r)\rangle \equiv |m_l,m_r\rangle \otimes |\Psi_0\rangle$ are degenerate. The first-order perturbative corrections to the ground-state energy E_0 are zero, but the second-order corrections are given by the eigenvalues of the matrix

$$V_{m_l,m_r;m_l',m_r'} = \sum_e \frac{\langle g(m_l,m_r)|H_{lr}|e\rangle\langle e|H_{lr}|g(m_l',m_r')\rangle}{E_0 - E_i},$$

where the summation spans the excited states $|e\rangle \equiv |m_l'',m_r''\rangle \otimes |\Psi_i\rangle (i=1,\ldots,2^n-1)$. In terms of the raising and lowering operators $S^{\pm}=S^x \pm iS^y$ we have

$$(\mathbf{S}_i \cdot \mathbf{S}_j)_\Delta \equiv \frac{1}{2}\left(S_i^+ S_j^- + S_i^- S_j^+\right) + \Delta S_i^z S_j^z, \tag{A2}$$

and a little algebra shows that

$$\begin{aligned} V_{m_l,m_r;m_l',m_r'} = {} & \frac{1}{4} J_l J_r \langle m_l,m_r|S_l^+ S_r^-|m_l',m_r'\rangle \sum_{i\neq 0} \frac{\langle\Psi_0|S_1^-|\Psi_i\rangle\langle\Psi_i|S_n^+|\Psi_0\rangle + \langle\Psi_0|S_n^+|\Psi_i\rangle\langle\Psi_i|S_1^-|\Psi_0\rangle}{E_0 - E_i} \\ & + \frac{1}{4} J_l J_r \langle m_l,m_r|S_l^- S_r^+|m_l',m_r'\rangle \sum_{i\neq 0} \frac{\langle\Psi_0|S_1^+|\Psi_i\rangle\langle\Psi_i|S_n^-|\Psi_0\rangle + \langle\Psi_0|S_n^-|\Psi_i\rangle\langle\Psi_i|S_1^+|\Psi_0\rangle}{E_0 - E_i} \\ & + \Delta_l \Delta_r J_l J_r \langle m_l,m_r|S_l^z S_r^z|m_l',m_r'\rangle \sum_{i\neq 0} \frac{\langle\Psi_0|S_1^z|\Psi_i\rangle\langle\Psi_i|S_n^z|\Psi_0\rangle + \langle\Psi_0|S_n^z|\Psi_i\rangle\langle\Psi_i|S_1^z|\Psi_0\rangle}{E_0 - E_i}. \end{aligned} \tag{A3}$$

Since the first two terms on the right-hand side of Eq. (A3) are complex conjugates, and noting that $E_0 - E_i$ is proportional to J_0, we can write

$$\begin{aligned} V_{m_l,m_r;m_l',m_r'} = {} & \gamma_n \frac{J_l J_r}{J_0} \langle m_l,m_r|S_l^x S_r^x + S_l^y S_r^y|m_l',m_r'\rangle \\ & + \gamma_n \delta_n \Delta_l \Delta_r \frac{J_l J_r}{J_0} \langle m_l,m_r|S_l^z S_r^z|m_l',m_r'\rangle, \end{aligned}$$

where γ_n and δ_n depend on Δ_0 [with $\delta_n=1$ for $\Delta_0=1$, where SU(2) symmetry is recovered]. The above matrix elements are precisely the ones corresponding to the Hamiltonian

$$H' = J'(S_l^x S_r^x + S_l^y S_r^y + \Delta' S_l^z S_r^z),$$

with the effective parameters J' and Δ' given by

$$J' = \gamma_n \frac{J_l J_r}{J_0} \quad \text{and} \quad \Delta' = \delta_n \Delta_l \Delta_r. \tag{A4}$$

For two-spin blocks we have

$$\gamma_2 = \frac{1}{1+\Delta_0} \quad \text{and} \quad \delta_2 = \frac{1+\Delta_0}{2}.$$

For larger blocks the parameters can be evaluated numerically as a function of Δ_0; however, for four-spin blocks we can analytically determine $\gamma_4=1$ in the *XX* limit and $\gamma_4=\frac{2}{3}-\sqrt{3}/6\simeq 0.378$ in the Heisenberg chain.

If n is odd (as in the three-spin case shown in Fig. 23), H_0 has two degenerate ground states, which we denote by $|\Psi_0^{\pm}\rangle$. These can be associated with an effective spin-$\frac{1}{2}$ S_0, whose states can be described by the azimuthal quantum number m_0, so that $|m_0=\pm\frac{1}{2}\rangle = |\Psi_0^{\pm}\rangle$. In the space $\mathbb{H}$ spanned by the states of S_0, S_l, and S_r, the states $|m_l,m_r,m_0\rangle \equiv |m_l\rangle \otimes |m_r\rangle \otimes |m_0\rangle$ are degenerate. The introduction of H_{lr} lifts this degeneracy, and we expect that, to order $J_{l,r}/J_0$, perturbation theory leads to an effective Hamiltonian H', with matrix elements given (apart from a constant) by

$$H'_{m_l,m_r,m_0;m_l',m_r',m_0'} = \langle m_l,m_r,m_0|H_{lr}|m_l',m_r',m_0'\rangle.$$

Restricting ourselves to the space $\mathbb{H}$, it is possible to write

$$H' = J_l'(\mathbf{S}_l \cdot \mathbf{S}_0)_{\Delta_l'} + J_r'(\mathbf{S}_0 \cdot \mathbf{S}_r)_{\Delta_r'},$$

provided

$$J_l(\mathbf{S}_l \cdot \mathbf{S}_1)_{\Delta_l} = J_l'(\mathbf{S}_l \cdot \mathbf{S}_0)_{\Delta_l'}, \tag{A5}$$

and

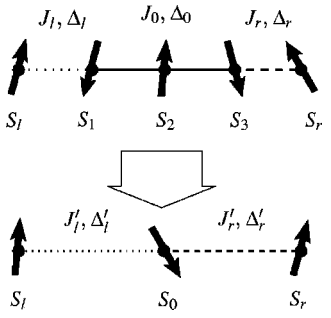

FIG. 23. Renormalization step involving a three-spin block.

$$J_r(\mathbf{S}_n \cdot \mathbf{S}_r)_{\Delta_r} = J'_r(\mathbf{S}_0 \cdot \mathbf{S}_r)_{\Delta'_r}.$$

We now expand Eq. (A5) with the help of Eq. (A2), and notice that

$$\langle m_l, m_r, m_0|S_l^+ S_0^-|m'_l, m'_r, m'_0\rangle = \delta_{m'_l, m_l-1}\delta_{m'_r, m_r}\delta_{m'_0, m_0+1},$$

$$\langle m_l, m_r, m_0|S_l^+ S_1^-|m'_l, m'_r, m'_0\rangle = \delta_{m'_l, m_l-1}\delta_{m'_r, m_r}\langle m_0|S_1^-|m'_0\rangle,$$

$$\langle m_l, m_r, m_0|S_l^z S_0^z|m'_l, m'_r, m'_0\rangle = m_l m_0 \delta_{m'_l, m_l}\delta_{m'_r, m_r}\delta_{m'_0, m_0},$$

$$\langle m_l, m_r, m_0|S_l^z S_1^z|m'_l, m'_r, m'_0\rangle = m_l \delta_{m'_l, m_l}\delta_{m'_r, m_r}\langle m_0|S_1^z|m'_0\rangle,$$

$\delta_{i,j}$ being the Kronecker symbol. By the Wigner-Eckart theorem, we can write

$$\langle m_0|S_1^-|m'_0\rangle = \gamma_n \delta_{m'_0, m_0+1},$$

$$\langle m_0|S_1^z|m'_0\rangle = (\delta_n \gamma_n) m_0 \delta_{m'_0, m_0},$$

with γ_n and δ_n depending on Δ_0, and we formally obtain the renormalized parameters,

$$J'_l = \gamma_n J_l \quad \text{and} \quad \Delta'_l = \delta_n \Delta_l. \tag{A6}$$

Analogously, by symmetry we have

$$J'_r = \gamma_n J_r \quad \text{and} \quad \Delta'_r = \delta_n \Delta_r. \tag{A7}$$

For three-spin blocks we obtain

$$\gamma_3 = \frac{\left(\Delta_0 + \sqrt{\Delta_0^2 + 8}\right)}{2 + \frac{1}{4}\left(\Delta_0 + \sqrt{\Delta_0^2 + 8}\right)^2},$$

and

$$\delta_3 = \frac{1}{4}\left(\Delta_0 + \sqrt{\Delta_0^2 + 8}\right),$$

while for larger blocks the parameters can be calculated numerically. In particular, for five-spin blocks we have, in the XX limit (for which analytical results are available), $\gamma_5 = \sqrt{3}/3 \simeq 0.577$, and in the Heisenberg chain $\gamma_5 \simeq 0.512$.

In blocks with an odd number of spins, the original spins S_i $(i=1,\ldots,n)$ are represented by the effective spin S_0, with "weights" given by the coefficients $c_{i,n}^x$ and $c_{i,n}^z$, defined through the operator identities (valid in $\mathbb{H}$)

$$S_i^x = c_{i,n}^x S_0^x \quad \text{and} \quad S_i^z = c_{i,n}^z S_0^z.$$

These are useful in the calculation of correlation functions. Note that $c_{1,n}^x = c_{n,n}^x = \gamma_n$ and $c_{1,n}^z = c_{n,n}^z = \delta_n \gamma_n$. For three-spin blocks we have

$$c_{2,3}^x = -\frac{1}{1 + \frac{1}{8}\left(\Delta_0 + \sqrt{\Delta_0^2 + 8}\right)^2},$$

and

$$c_{2,3}^z = \frac{1}{4}\Delta_0\left(\Delta_0 + \sqrt{\Delta_0^2 + 8}\right)c_{2,3}^x.$$

Equations (A4), (A6), and (A7) constitute the recursion relations defining the RG steps in the MDH scheme.

APPENDIX B: SECOND-ORDER CALCULATION OF CORRELATION FUNCTIONS

Let us assume that a two-spin block, such as the one shown in Fig. 22, is selected for renormalization at some point of the RG process. In terms of the states of S_1 and S_2, the eigenstates of the block Hamiltonian H_0, with the corresponding energies, are

$$|\Psi_0\rangle = \frac{1}{\sqrt{2}}(|\uparrow\downarrow\rangle - |\downarrow\uparrow\rangle), \quad E_0 = -\left(\frac{1}{2} + \frac{1}{4}\Delta_0\right)J_0,$$

$$|\Psi_1\rangle = |\uparrow\uparrow\rangle, \quad |\Psi_2\rangle = |\downarrow\downarrow\rangle, \quad E_1 = E_2 = \frac{1}{4}\Delta_0 J_0,$$

and

$$|\Psi_3\rangle = \frac{1}{\sqrt{2}}(|\uparrow\downarrow\rangle + |\downarrow\uparrow\rangle), \quad E_3 = \left(\frac{1}{2} - \frac{1}{4}\Delta_0\right)J_0.$$

The connection between the two-spin block and the rest of the chain, through the neighboring spins S_l and S_r, is described by the Hamiltonian H_{lr} in Eq. (A1).

Denoting by $|A_i\rangle$ the states of all other spins in the chain, and assuming that in the thermodynamic limit there is a unique ground state $|A_0\rangle$, the ground state of the whole chain can be written, at the zeroth order in perturbation theory, as $|g_0\rangle = |A_0, \Psi_0\rangle$. Up to the second order in $J_{l,r}/J_0$ we obtain a corrected state,

$$\begin{aligned}|g\rangle = |g_0\rangle &+ \sum_i \sum_{k\neq 0} |A_i, \Psi_k\rangle \frac{\langle A_i, \Psi_k|H_{lr}|A_0, \Psi_0\rangle}{E_0 - E_k} \\ &+ \sum_{i,j} \sum_{k,\ell\neq 0} |A_i, \Psi_k\rangle \frac{\langle A_i, \Psi_k|H_{lr}|A_j, \Psi_\ell\rangle\langle A_j, \Psi_\ell|H_{lr}|A_0, \Psi_0\rangle}{(E_0 - E_k)(E_0 - E_\ell)} \\ &- \sum_{i,j} \sum_{k\neq 0} |A_i, \Psi_k\rangle \frac{\langle A_i, \Psi_k|H_{lr}|A_j, \Psi_0\rangle\langle A_j, \Psi_0|H_{lr}|A_0, \Psi_0\rangle}{(E_0 - E_k)^2}.\end{aligned} \tag{B1}$$

A second-order estimate of the expectation value of any operator O is simply given by

$$\langle O\rangle_g \equiv \frac{\langle g|O|g\rangle}{\langle g|g\rangle}.$$

For the calculation of correlation functions involving spins in the block, we write $O = O_\Psi O_A$, where O_Ψ and O_A are operators acting on the subspaces defined by the states $|\Psi_i\rangle$ and $|A_i\rangle$, respectively. Expanding Eq. (B1), we obtain an expression for $\langle g|O|g\rangle$ with terms containing combinations such as $\langle\Psi_i|O_\Psi|\Psi_j\rangle$ and $\langle A_0|S_l^+ O_A|A_0\rangle$, which is rather cumbersome to write here. As examples of the final results obtained in the Heisenberg limit, we have

$$\langle g|g\rangle \equiv g^{-1} = 1 + \frac{3}{16}\frac{J_l^2 + J_r^2}{J_0^2} - \frac{1}{2}\frac{J_l J_r}{J_0^2}\langle A_0|\mathbf{S}_l \cdot \mathbf{S}_r|A_0\rangle,$$

$$\langle \mathbf{S}_1 \cdot \mathbf{S}_2 \rangle_g = -\frac{3}{4} g \left(1 - \frac{1}{16} \frac{J_l^2 + J_r^2}{J_0^2} + \frac{1}{6} \frac{J_l J_r}{J_0^2} \langle A_0 | \mathbf{S}_l \cdot \mathbf{S}_r | A_0 \rangle \right),$$

$$\langle \mathbf{S}_l \cdot \mathbf{S}_1 \rangle_g = \frac{1}{2} g \left[\left(\frac{1}{3} + \frac{1}{4} \frac{J_r + 2J_l}{J_0} \right) \frac{J_r}{J_0} \langle A_0 | \mathbf{S}_l \cdot \mathbf{S}_r | A_0 \rangle - \frac{1}{4} \left(1 + \frac{3}{4} \frac{J_l}{J_0} \right) \frac{J_l}{J_0} \right],$$

and

$$\langle \mathbf{S}_n \cdot \mathbf{S}_1 \rangle_g = -\frac{1}{2} g \left[\left(1 + \frac{1}{4} \frac{J_l}{J_0} \right) \frac{J_l}{J_0} \langle A_0 | \mathbf{S}_n \cdot \mathbf{S}_l | A_0 \rangle - \left(1 + \frac{3}{4} \frac{J_r}{J_0} \right) \frac{J_r}{J_0} \langle A_0 | \mathbf{S}_n \cdot \mathbf{S}_r | A_0 \rangle \right],$$

S_n being any spin other than S_l, S_r, S_1 and S_2. These expressions depend explicitly on expectation values like $\langle A_0 | \mathbf{S}_l \cdot \mathbf{S}_r | A_0 \rangle$, which in turn depend on expectation values involving spins neighboring the blocks in which S_l and S_r will be decimated. As the RG proceeds, this generates a hierarchical structure, which can be solved backwards by assuming that the correlation between the spins in the very last block to be renormalized takes it zeroth-order value. It is interesting to notice that the correlation between two spins which are not decimated in the same block is at most of order $J_{l,r}/J_0$.

Similarly, in the *XX* limit we have, for instance,

$$\langle g | g \rangle \equiv g^{-1} = 1 + \frac{1}{2} \frac{J_l^2 + J_r^2}{J_0^2} - 4 \frac{J_l J_r}{J_0^2} \langle A_0 | S_l^x S_r^x | A_0 \rangle,$$

$$\langle S_1^x S_2^x \rangle_g = -\frac{1}{4} g,$$

$$\langle S_1^z S_2^z \rangle_g = -\frac{1}{4} g \left(1 - \frac{1}{2} \frac{J_l^2 + J_r^2}{J_0^2} + 4 \frac{J_l J_r}{J_0^2} \langle A_0 | S_l^x S_r^x | A_0 \rangle \right),$$

$$\langle S_n^x S_{1,2}^x \rangle_g = -g \left(\frac{J_{l,r}}{J_0} \langle A_0 | S_n^x S_{l,r}^x | A_0 \rangle - \frac{J_{r,l}}{J_0} \langle A_0 | S_n^x S_{r,l}^x | A_0 \rangle \right),$$

$$\langle S_n^z S_{1,2}^z \rangle_g = g \frac{J_{r,l}^2}{J_0^2} \langle A_0 | S_n^z S_{r,l}^z | A_0 \rangle.$$

Notice that expressions for the *zz* correlations may involve other expectation values of both *xx* and *zz* correlations.

*Electronic address: apvieira@if.usp.br

[1] D. S. Fisher, Phys. Rev. Lett. **69**, 534 (1992).
[2] D. S. Fisher, Phys. Rev. B **51**, 6411 (1995).
[3] A. Furusaki, M. Sigrist, P. A. Lee, K. Tanaka, and N. Nagaosa, Phys. Rev. Lett. **73**, 2622 (1994).
[4] A. Furusaki, M. Sigrist, E. Westerberg, P. A. Lee, K. B. Tanaka, and N. Nagaosa, Phys. Rev. B **52**, 15 930 (1995).
[5] T. N. Nguyen, P. A. Lee, and H.-C. zur Loye, Science **271**, 489 (1996).
[6] E. Westerberg, A. Furusaki, M. Sigrist, and P. A. Lee, Phys. Rev. Lett. **75**, 4302 (1995).
[7] E. Westerberg, A. Furusaki, M. Sigrist, and P. A. Lee, Phys. Rev. B **55**, 12 578 (1997).
[8] D. S. Fisher, Phys. Rev. B **50**, 3799 (1994).
[9] G. Refael, S. Kehrein, and D. S. Fisher, Phys. Rev. B **66**, 060402(R) (2002).
[10] M. Kohmoto, L. P. Kadanoff, and C. Tang, Phys. Rev. Lett. **50**, 1870 (1983).
[11] J. M. Luck and T. Nieuwenhuizen, Europhys. Lett. **2**, 257 (1986).
[12] J. M. Luck, J. Stat. Phys. **72**, 417 (1993).
[13] J. Vidal, D. Mouhanna, and T. Giamarchi, Phys. Rev. Lett. **83**, 3908 (1999).
[14] J. Vidal, D. Mouhanna, and T. Giamarchi, Phys. Rev. B **65**, 014201 (2001).
[15] K. Hida, J. Phys. Soc. Jpn. **68**, 3177 (1999).
[16] K. Hida, Phys. Rev. Lett. **86**, 1331 (2001).
[17] J. Hermisson, J. Phys. A **33**, 57 (2000).
[18] M. Arlego, D. C. Cabra, and M. D. Grynberg, Phys. Rev. B **64**, 134419 (2001).
[19] D. Shechtman, I. Blech, D. Gratias, and J. W. Cahn, Phys. Rev. Lett. **53**, 1951 (1984).
[20] For recent results on two-dimensional antiferromagnetic quasicrystals see S. Wessel, A. Jagannathan, and S. Haas, Phys. Rev. Lett. **90**, 177205 (2003) and also A. Jagannathan, *ibid.* **92**, 047202 (2004).
[21] R. J. Baxter, Ann. Phys. (N.Y.) **70**, 193 (1972).
[22] A. Luther and I. Peschel, Phys. Rev. B **12**, 3908 (1975).
[23] M. C. Cross and D. S. Fisher, Phys. Rev. B **19**, 402 (1979).
[24] J. C. Bonner and H. W. J. Blöte, Phys. Rev. B **25**, 6959 (1982).
[25] T. Barnes, J. Riera, and D. A. Tennant, Phys. Rev. B **59**, 11 384 (1999).
[26] S.-K. Ma, C. Dasgupta, and C.-K. Hu, Phys. Rev. Lett. **43**, 1434 (1979).
[27] C. Dasgupta and S.-K. Ma, Phys. Rev. B **22**, 1305 (1980).
[28] R. A. Hyman, K. Yang, R. N. Bhatt, and S. M. Girvin, Phys. Rev. Lett. **76**, 839 (1996).
[29] P. Le Doussal, C. Monthus, and D. S. Fisher, Phys. Rev. E **59**, 4795 (1999).
[30] A. Saguia, B. Boechat, and M. A. Continentino, Phys. Rev. Lett. **89**, 117202 (2002).
[31] E. Yusuf and K. Yang, Phys. Rev. B **65**, 224428 (2002).
[32] J. A. Hoyos and E. Miranda, Phys. Rev. B **69**, 214411 (2004).
[33] J. Hooyberghs, F. Iglói, and C. Vanderzande, Phys. Rev. Lett. **90**, 100601 (2003).
[34] J. A. Hoyos and E. Miranda, Phys. Rev. B **70**, 180401(R) (2004).
[35] A. Janner and T. Janssen, Phys. Rev. B **15**, 643 (1977).
[36] V. Elser, Phys. Rev. B **32**, 4892 (1985).
[37] There are, however, cases where a substitution rule generates a periodic sequence, as in $a \to ab$, $b \to ab$. It is possible to establish conditions under which a substitution rule generates an aperiodic sequence; see, e.g., S. T. R. Pinho and T. C. P. Lobão, Braz. J. Phys. **30**, 772 (2000).

[38] C. Godrèche and J. M. Luck, Phys. Rev. B **45**, 176 (1992).
[39] K. Hida, Phys. Rev. Lett. **93**, 037205 (2004).
[40] K. Hida, J. Phys. Soc. Jpn. **73**, 2296 (2004).
[41] A. P. Vieira, Phys. Rev. Lett. **94**, 077201 (2005).
[42] N. Laflorencie and H. Rieger, Phys. Rev. Lett. **91**, 229701 (2003).
[43] C. A. Doty and D. S. Fisher, Phys. Rev. B **45**, 2167 (1992).
[44] M. Queffélec, *Substitution Dynamical Systems-Spectral Analysis*, Lecture Notes in Mathematics, Vol. 1294 (Springer-Verlag, Berlin, 1987).
[45] J. M. Luck, C. Godrèche, A. Janner, and T. Janssen, J. Phys. A **26**, 1951 (1993).
[46] A. B. Harris, J. Phys. C **7**, 1671 (1974).
[47] J. M. Luck, Europhys. Lett. **24**, 359 (1993).
[48] T. C. Lubensky, Phys. Rev. B **11**, 3573 (1975).
[49] P. T. Muzy, A. P. Vieira, and S. R. Salinas, Phys. Rev. E **65**, 046120 (2002).
[50] E. Lieb, T. Schultz, and D. Mattis, Ann. Phys. **16**, 407 (1961).
[51] P. Pfeuty, Phys. Lett. **72A**, 245 (1979).
[52] Q. Niu and F. Nori, Phys. Rev. Lett. **57**, 2057 (1986).
[53] D. Barache and J. M. Luck, Phys. Rev. B **49**, 15 004 (1994).
[54] N. Fujita and K. Niizeki, Phys. Rev. Lett. **85**, 4924 (2000).
[55] The presence of two-cycles in association with aperiodicity is not uncommon. In ferromagnetic q-state Potts models with a suitable choice of aperiodic couplings, for sufficiently large q the finite-temperature critical behavior is governed by a two-cycle, the uniform fixed point being unstable; see, e.g., T. A. S. Haddad, S. T. R. Pinho, and S. R. Salinas, Phys. Rev. E **61**, 3330 (2000).
[56] J. M. Luck, Phys. Rev. B **39**, 5834 (1989).
[57] M. Arlego, Phys. Rev. B **66**, 052419 (2002).
[58] F. Iglói, D. Karevski, and H. Rieger, Eur. Phys. J. B **1**, 513 (1998).
[59] F. Iglói, D. Karevski, and H. Rieger, Eur. Phys. J. B **5**, 613 (1998).
[60] R. B. Griffiths, Phys. Rev. Lett. **23**, 17 (1969).
[61] E. Lieb and D. Mattis, J. Math. Phys. **3**, 749 (1962).